RESEARCH

Study on shoreline migration and island dynamics over the last five decades in the Muriganga River using multi-temporal satellite images

Md Saddam Hossain · Ujjwal Saha

Abstract The Muriganga River, also known as channel creek, underwent morphological changes often since it is an alluvial as well as a tidal river. The present study analyses the morphological changes in the Muriganga River and its islands with the help of the Remote Sensing and Geographical Information System (GIS) and digital shoreline analysis tool (DSAS 5.0). Moreover, the computation of morphological changes was also performed on two islands, i.e. Sagar and Ghoramara, which are situated just outside the river reach. Eight cloud-free satellite images of Landsat MSS (1972–1980), Landsat TM (1988–2011) and Landsat OLI (2017–2021) have been used to investigate the river shoreline shifting and island dynamics of the Muriganga River resulted from the erosion–accretion process during the last 49 years. For the short-term study, the erosion–accretion rates are derived from one Landsat image to the next, whereas for long-term analysis, the erosion–accretion rates are estimated based on the difference between 1972 as the reference image and the succeeding images. Short-term and long-term analysis shows that the average rate of erosion is more than that of accretion in Muriganga River. It is also found that the areas of Sagar, Ghoramara, Mousuni and Pushpa islands are shrinking continuously, whereas the Niogi and Basit islands are expanding enormously. These may indicate that the shoreline erosion results in widening the river and the eroded materials are accumulated in Niogi and Basit islands. The results suggest that there is an urge for a better coastal management strategy for the erosion control scheme. This study also helps in gaining knowledge of maintaining the navigability in the Muriganga River.

Keywords Shoreline migration · Island dynamics · Muriganga River · Multi-temporal satellite images · NDWI

Introduction

One of the most dynamic regions of the earth's surface is its coasts. The term "coastal zone" refers to a large geographic region where the interaction of terrestrial and marine forces results in distinctive biological systems and landforms (Jayappa et al., 2006). Short-term and long-term shoreline alterations are influenced by several types of factors such as sea-level rise, interaction of coastline with river mouth, tidal currents, wind intensity wave height and sediment supply (Ding & Wang, 2008; Hakkou et al., 2018; Kumar & Jayappa, 2009). Several physical processes, such as erosionsedimentation, tidal flooding,

M. S. Hossain (✉) · U. Saha
Civil Engineering Department, Indian Institute of Engineering Science and Technology, Shibpur, Howrah 711103, India
e-mail: mdsad00728@gmail.com

U. Saha
e-mail: ujjwalsaha1980@gmail.com

land subsidence, volcanic activity and sea-level rise, are constantly causing both slow and abrupt changes (Maiti & Bhattacharya, 2009) in a coastal environment. The coasts have always been subjected to erosion and accretion caused by wave action, tsunamis, storm surges, floods, cyclones, sea-level rise, tide and wind variations (Mukhopadhyay et al., 2011). Anthropogenic activities like dredging of tidal entrances and navigational channels, construction of harbours and jetties, river water regulation works, hardening of shorelines with seawalls, destruction of mangroves and other natural buffers and beach sand mining increase the process of changes in shoreline (Dilara & Tarik, 2019; Jayakumar & Malarvannan, 2016). The shoreline shifting process is categorized as eroding, i.e. landward movement, equilibrium, i.e. stable and accreting, i.e. seaward movement (Salghuna & Bharathvaj, 2015). The strength of the bank materials plays an important role in the movement of the shoreline (Knighton, 1984; Morisawa & Hack, 1985). The climatic, geomorphic, tectonic and hydrodynamic forces influence both long-term and short-term shoreline change phenomena (Bagli & Soille, 2003; Marfai & Almohammad, 2008; McBride et al., 1995; Mills et al., 2005; Scott, 2005; Sunarto, 2004; Thom & Cowell, 2005).

In the past, when performing surveys was regarded to be the most accurate way to undertake earth science research, substantial field and measuring work was done to determine the ground position of coastlines. However, human mistake causes unsystematic errors that are difficult to correct (Wright & Coleman, 1973). It is hard to undertake a ground survey in an unstable fluvial environment. However, remote sensing techniques combined with GIS techniques offer spatial information (Broers et al., 1990; Dépret et al., 2017; Dixon et al., 2018; Hassan et al., 1999; Islam, 2000; Marcus & Fonstad, 2010; Mount et al., 2013; Roberts et al., 1993; Sarker & Thorne, 2009). This technique is better suited for monitoring deltaic and coastal areas than traditional approaches (Muthusankar, 2011; Saranathan et al., 2011). The spatial and temporal analyses of different rivers in various regions of the world have been studied using remote sensing (RS) and GIS techniques. With the help of the digital shoreline analysis system (DSAS), the linear regression rate (LRR), the end point rate (EPR) and the

net shoreline movement (NSM) can be easily calculated by using the multi-temporal satellite images. Numerous researchers (Thieler et al., 2009; Mujabar & Chandrasekar, 2011; Hakkou et al., 2018; Karim Nassar et al., 2018; Natarajan et al., 2021; Chrisben Sam & Gurugnanam, 2022; Aladwani, 2022) have successfully used multi-temporal satellite images of Landsat MSS, Landsat TM, Landsat ETM and Landsat OLI to detect the shoreline changes in Kenitra coast (Morocco), in the coast of northern Sinai (Egypt), southeast coast of Cuddalore (India), coastal tip of Peninsular (India) and southern coast of Kuwait, respectively.

Human livelihoods close to the riverbank are in danger from ongoing erosion; on the other side, accretion in the riverbed is causing the construction of permanent shallow reefs or islands, and therefore, fish and aquatic species are decreasing considerably. The main concern of the people living near the bank line depends on the stability and vulnerability of that bank line. The rising and falling stages of flood have a significant impact on the stability of the shoreline. Therefore, it is essential to investigate and analyse the shoreline position to determine how vulnerable the coast is, which helps the engineers in better coastal management planning, hazard zone mapping, sea–water intrusion and so on.

The main objective of this study is to analyse the erosion–accretion changes during the last five decades in the Muriganga River as well as in Sagar and Ghoramara islands. From the analysis, it is found that both the left bank and right bank are subjected to erosion. Sagar and Ghoramara islands are gradually losing their area. Some islands like Mousuni and Pushpa are shrinking their area due to continuous erosion, whereas islands like Niogi and Basit are incessantly expanding their land due to continuous accretion. Though the Half-fish island is constantly eroding till 2004, it started expanding its area from 2004 onward. This may indicate that the locally eroded materials from Mousuni island, Pushpa island and banks get deposited at Niogi and Basit island. It is essential to know how the dynamic behaviour of the islands and river has changed from 1972 to 2021. Therefore, this analysis will be helpful in understanding the shoreline migration and island dynamics which may help the coastal engineers to prepare better coastal management plans.

Study area

Muriganga River is a distributary of river Hooghly. The river is also known as Bartala and is located in the district of South 24 Parganas of West Bengal. The river is confined by the latitude between 21°34′30″ N to 21°57′30″ N and longitude between 88°02′00″ E to 88°15′00″ E (Fig. 1). The Hooghly river bifurcates at the northern tip of Sagar island. The western part remains as Hooghly, and the eastern part is named as the Muriganga River also known as Hooghly channel creek. The Muriganga River is an alluvial as well as a tidal river of the Hooghly estuary system. The estuary's shape has an impact on making the land shape. Hence, the funnel shape of the estuary makes the tides asymmetric in nature. Because of this, high tide enters the estuary, while low tide cannot propagate properly. This fluctuation of flow is one of the primary reasons for the change in shoreline in that region. The Sagar island has an average elevation of 6.5 m above mean sea level (Mukherjee, 1983).

Materials and methods

To study the morphological changes in the Muriganga River as well as at Sagar island and Ghoramara island, eight cloud-free Landsat (MSS, TM and OLI-TIRS) satellite images of different years between 1972 and 2021 are collected from the US Geological Survey (USGS) Earth Explorer. The details of the Landsat satellite images used in this study are shown in Table 1. In this study, the ArcGIS 10.4 tool has been used to calculate the geomorphological changes in the river and in the islands. The visual interpretation may be performed to digitize the shoreline. But there may have some errors. Hence, the normalized difference water index (NDWI) was calculated to differentiate
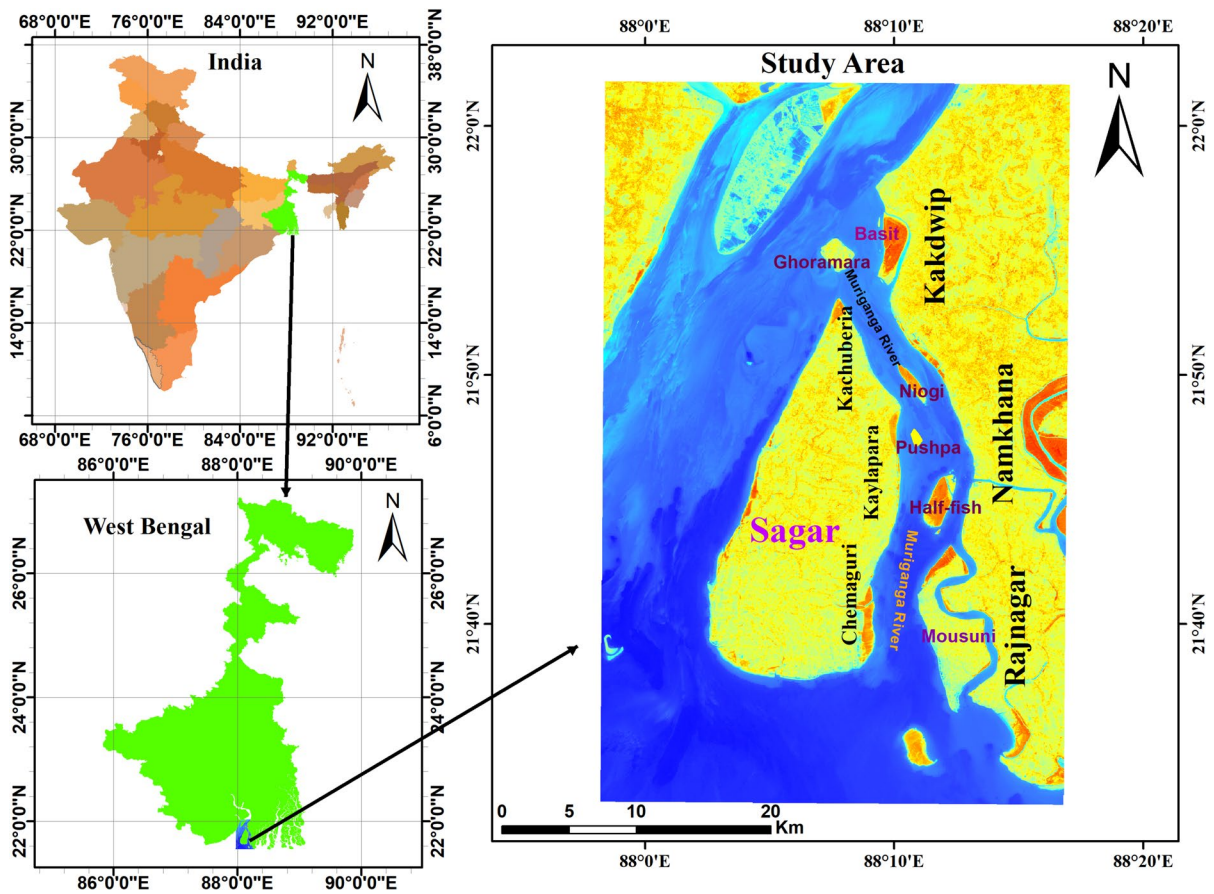

Fig. 1 Location map showing the Muriganga River, Sagar island and Ghoramara island

Table 1 Details of the Landsat images used in this study

Sl No.	Data source and sensor	Date of acquisition (DD/MM/YYYY)
1	Landsat 1 MSS	12/12/1972
2	Landsat 3 MSS	21/02/1980
3	Landsat 5 TM	26/12/1988
4	Landsat 5 TM	16/02/1996
5	Landsat 5 TM	22/12/2004
6	Landsat 5 TM	25/02/2011
7	Landsat 8 OLI_TIRS	24/01/2017
8	Landsat 8 OLI_TIRS	21/12/2021

the water body and land. NDWI index is a satellite-derived index and is calculated as the normalized difference between green and near-infrared bands based on per-pixel value (McFeeters, 1996). Band 4 and band 2 of Landsat TM are considered near-infrared (NIR) and green, respectively. Landsat MSS consists of 4 bands (4, 5, 6 and 7), and it is difficult to identify the exact band for NDWI calculation. Therefore, bands 4 and 6 here are used as green and NIR.

For NDWI analysis with the help of ArcGIS, the following Eq. (1) is used for Landsat MSS, Eq. (2) is used for Landsat TM, and Eq. (3) is used for Landsat OLI_TIRS, respectively:

$$NDWI = \frac{Green - NIR}{Green + NIR} = \frac{Band\ 4 - Band\ 6}{Band\ 4 + Band\ 6} \quad (1)$$

$$NDWI = \frac{Green - NIR}{Green + NIR} = \frac{Band\ 2 - Band\ 4}{Band\ 2 + Band\ 4} \quad (2)$$

$$NDWI = \frac{Green - NIR}{Green + NIR} = \frac{Band\ 3 - Band\ 5}{Band\ 5 + Band\ 5} \quad (3)$$

For the calculation of the shoreline shifting rate, DSAS 5.0, an extension of ArcGIS, is used. There are mainly four steps involved in the computation of shoreline shifting, such as the creation of baseline, preparation of baseline, generation of transects and, finally, calculation of the rate of changes in the shoreline (Nithu et al., 2020). Initially, the date and time format of the computer is kept as mm/dd/yyyy and English (USA). A personal geodatabase is created in ArcGIS for performing DSAS Analysis. The digitized shorelines and baseline are in the projected coordinate system of m (such as UTM or State Plane). These digitized baselines and shorelines are added to a personal geodatabase. From the baseline, 2000-m transects are placed perpendicularly to the right bank shorelines of different years at an interval of 100 m with 250-m smoothing distance. On the other hand, 2000-m transects are placed perpendicularly to the left bank at an interval of 200 m with a smoothing distance of 250 m. A total of 304 and 264 transects were created for right bank and left bank, respectively. These transects feature data are used for the calculation of shoreline movement. In this analysis, some statistical techniques such as net shoreline movement (NSM), end point rate (EPR) and linear regression rate (LRR) are used. In terms of shoreline variation rates, accretion exhibited positive values, whereas erosion showed negative values.

The NSM estimates the actual distance between the oldest and youngest shorelines for each transect placed perpendicular to the shorelines (Himmelstoss et al., 2018). This is calculated as

$$NSM = \left\{ d_{2021} - d_{1972} \right\} m \quad (4)$$

For calculating the EPR, shoreline movement distance is divided by the time period between the oldest and most recent shoreline (Himmelstoss et al., 2018). The minimum requirements for EPR calculation are two shoreline dates as well as relevant information such as changes in sign (in other words, erosion and accretion), cyclical trends or magnitude, if such information is available (e.g. Crowell et al., 1997; Dolan et al., 1991). This is calculated as

$$EPR = \frac{d_{2021} - d_{1972}}{t_{2021} - t_{1972}} m/year \quad (5)$$

The linear regression rate (LRR) determines the rate of change by fitting the least squares regression line to all the points of shorelines of transect (Himmelstoss et al., 2018).

Results

Short-term and long-term river dynamics

In short-term analysis, the erosion–accretion is calculated from one Landsat image to the next subsequent image in temporal scale. But in long-term study, the erosion–accretion is calculated by taking

the difference between the Landsat image of 1972 as a reference and the next subsequent images. The rate of erosion and accretion in Muriganga River is given in Table 2. From the short-term and long-term analysis, it is found that the average short-term and long-term erosion rates during the period starting from 1972 to 2021 in the Muriganga River are 137.58 ha/year and 98.61 ha/year, respectively, whereas the average accretion rates are 82.60 ha/year and 26.98 ha/year, respectively. During this period, the overall erosion and accretion in the Muriganga River are found as 6368.82 ha and 4008.65 ha, respectively. The temporal evolution of the land areas of the islands and water area of the Muriganga River is shown in Fig. 2. Initially, the area of the Muriganga River was 14,029.42 ha in 1972, but in 2021, the area is 16,390.02 ha. Fig. 3 also indicates that the banks are gradually eroding, leading to the widening of the river. During 1996–2004 and 2004–2011 time periods, there is some accretion that took place within the river islands. The Niogi island evolved between 2004 and 2011, and there is a continuous expansion of Basit island from 1972 onwards. Otherwise, throughout the whole time period, the erosion is more than that of accretion which clearly shows that the water area is expanding enormously. The islands such as Pushpa and Mousuni which are situated at the lower region of the river are continuously eroding, whereas the islands such as Niogi and Basit, situated at the upper region of the river, are continuously accreting (Fig. 2) throughout this time period. But the Half-fish island is found to be very dynamic

because it gets eroded till 2004 and then started accreting till now (Fig. 2).

Short-term and long-term island dynamics

The notable islands within the Muriganga River are Basit, Niogi, Pushpa, Half-fish and Mousuni. The Sagar island is located at the western side of the river, whereas the Ghoramara island is situated near the entrance of the Muriganga River. From the short-term and long-term analysis, it is found that all the islands are highly dynamic in nature. Some islands, like Basit and Niogi, are getting accreted, while the remaining islands are getting eroded during the 1972 to 2021 time period.

Sagar island

Sagar island is one of the popular island in Hooghly estuary. The famous temple of Kapil Muni is located at the southern tip of Sagar island. Gangasagar Mela is regarded as one of the most popular fair which is celebrated in every year in this island. The Sagar island has lost a significant area of near about 9.26 % of its area from 25,874.80 (1972) to 23,476.62 ha (2021) (Fig. 2b). From short-term and long-term analysis, the average rate of erosion and accretion in Sagar island is 90.08 ha/year and 62.92 ha/year and 25.05 ha/year and 7.68 ha/year (Table 3), respectively. It clearly indicates that the average erosion rate is more pronounced than the accretion rate in Sagar island which causes the reduction in area. This island shows more accretion during 1996–2004 and 2004–2011 time periods in short-term analysis

Table 2 Short-term and long-term erosion accretion rate in Muriganga River

Short-term erosion accretion rate					Long-term erosion accretion rate				
Duration	Erosion		Accretion		Duration	Erosion		Accretion	
	Total (ha)	Rate (ha/y)	Total (ha)	Rate (ha/y)		Total (ha)	Rate (ha/y)	Total (ha)	Rate (ha/y)
1972–1980	1152.18	144.02	423.20	52.90	1972–1980	1152.18	144.02	423.20	52.90
1980–1988	1532.52	191.56	218.01	27.25	1972–1988	2177.46	136.09	133.98	8.37
1988–1996	704.47	88.06	187.60	23.45	1972–1996	2680.19	111.67	119.84	3.75
1996–2004	496.68	62.09	670.74	83.84	1972–2004	2923.68	91.36	537.39	16.79
2004–2011	153.27	21.90	2098.37	299.77	1972–2011	2409.85	61.79	1968.65	50.48
2011–2017	1523.66	253.94	140.73	23.46	1972–2017	3148.21	69.96	1324.08	29.42
2017–2021	806.04	201.51	270.00	67.50	1972–2021	3691.38	75.33	1331.21	27.17
Average		137.58		82.60			98.61		26.98

Fig. 2 Area of the Muriganga River (**a**), Sagar island (**b**), Ghoramara island (**c**), Mousuni island (**d**), Half-fish island (**e**), Pushpa island (**f**), Basit island (**g**) and Niogi island (**h**) in the different time periods
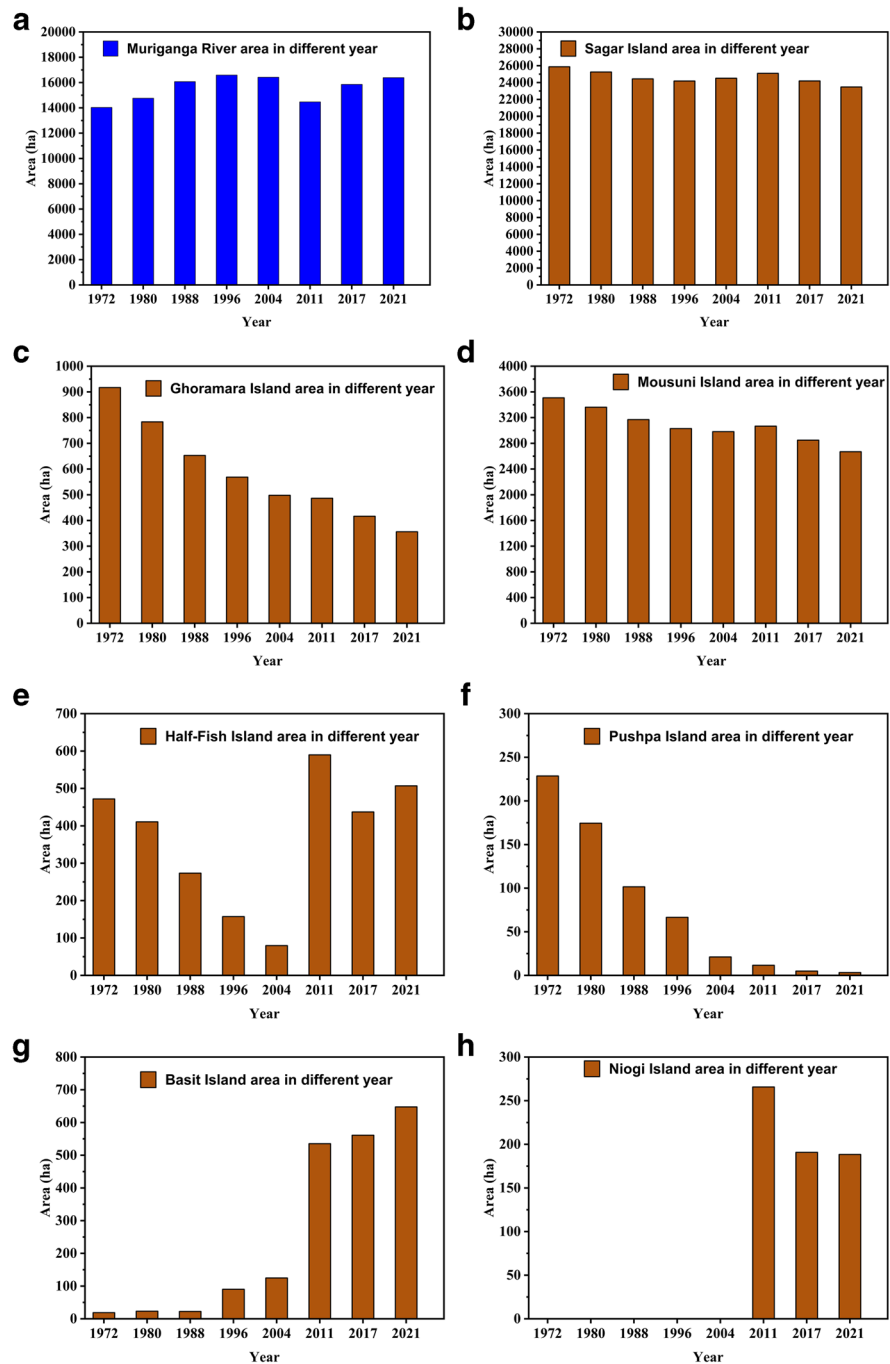
(Fig. 4b). But from the long-term point of view, the island is shrinking. Most of the erosion was taken place in the western side and in the southern side of the island (Fig. 4). Very popular and active navigational channels like Ranglafalla, Jelingham, Eden and Auckland are located in the western side of the Sagar island. Dredging is often done here in these channels to continuously maintain the navigability
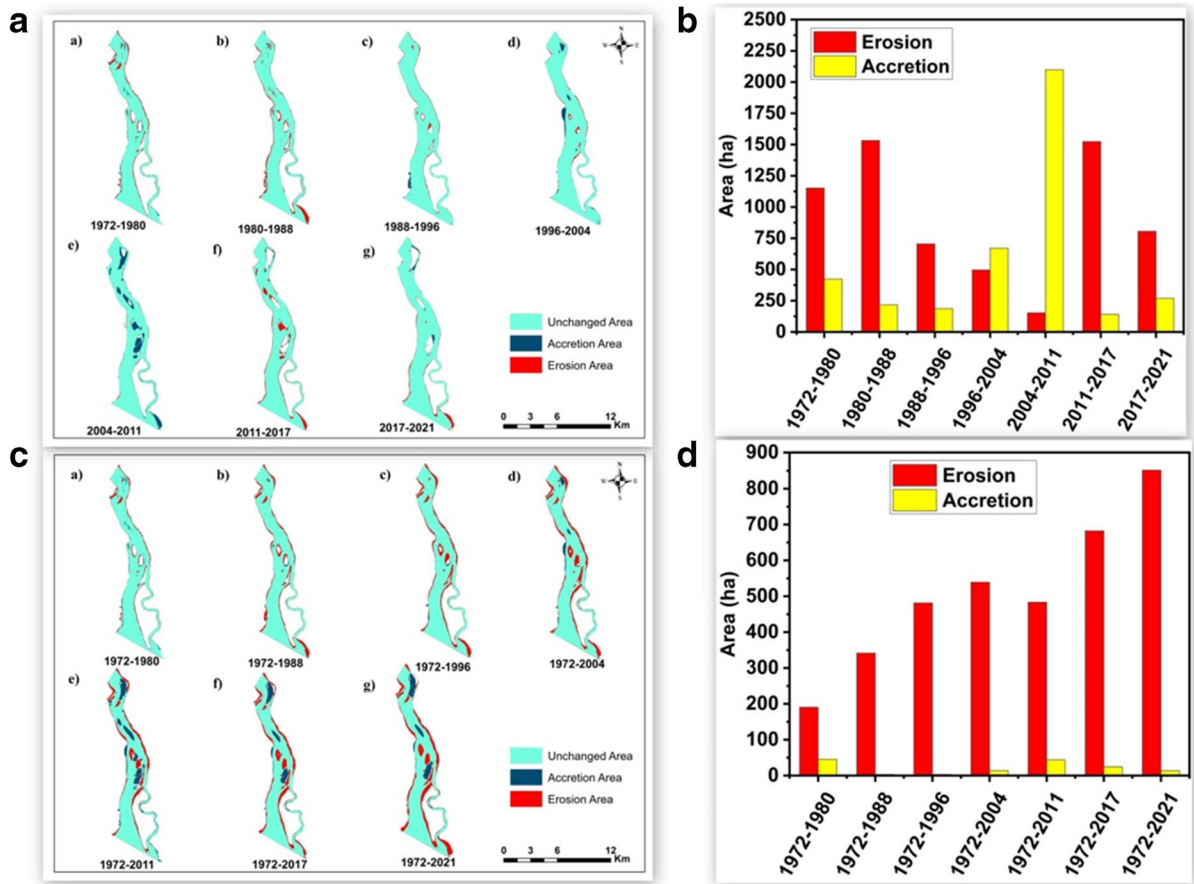
Fig. 3 Short-term erosion–accretion in the Muriganga River (**a** and **b**) and long-term erosion–accretion in the Muriganga River (**c** and **d**) (1:450,000 scale) during the different time periods from 1972 to 2021

Table 3 Short-term and long-term erosion accretion rate in Sagar island

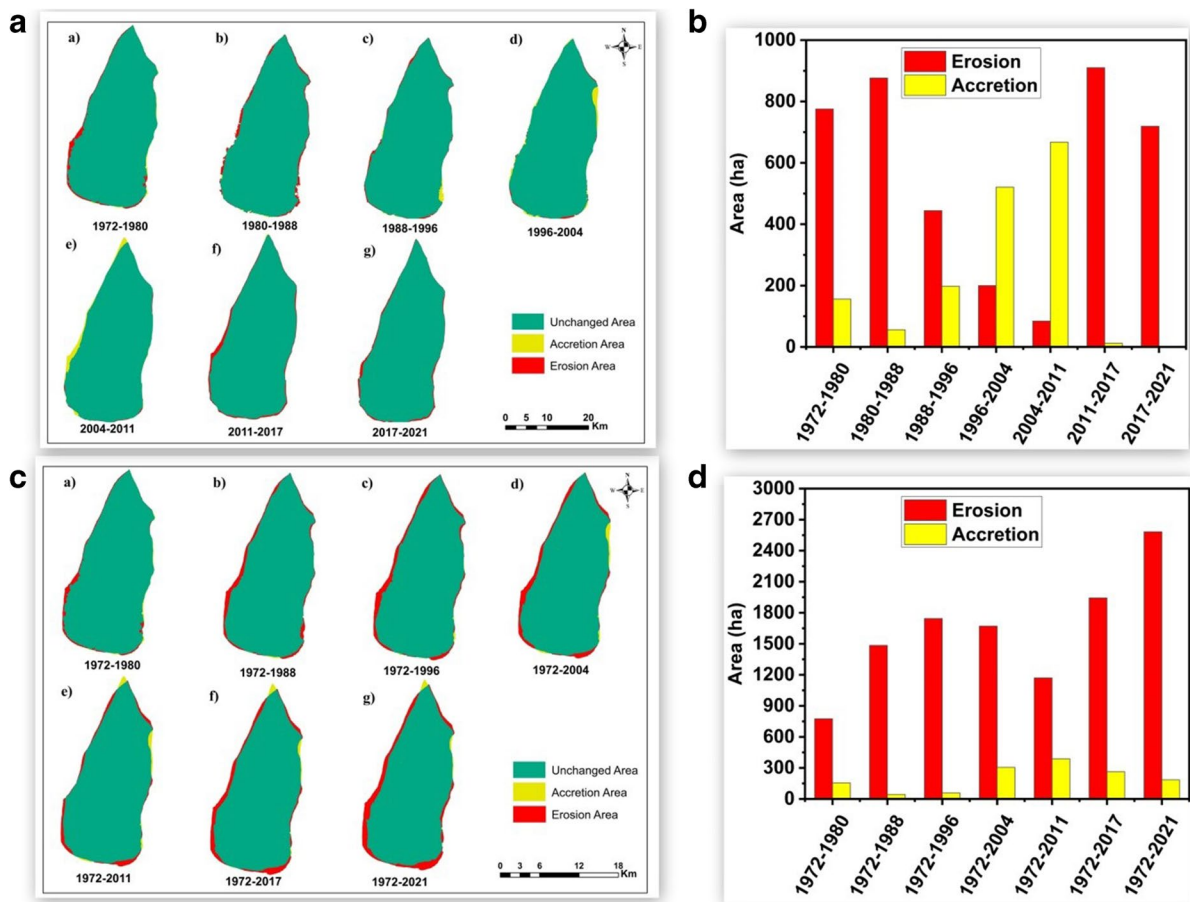| Short-term erosion accretion rate					Long-term erosion accretion rate				
Duration	Erosion		Accretion		Duration	Erosion		Accretion	
	Total (ha)	Rate (ha/y)	Total (ha)	Rate (ha/y)		Total (ha)	Rate (ha/y)	Total (ha)	Rate (ha/y)
1972–1980	775.45	96.93	155.89	19.49	1972–1980	775.45	96.93	155.89	19.49
1980–1988	876.45	109.56	55.87	6.98	1972–1988	1483.93	92.75	43.78	2.74
1988–1996	444.29	55.54	198.04	24.75	1972–1996	1744.21	72.68	57.81	2.41
1996–2004	199.84	24.98	520.90	65.11	1972–2004	1670.63	52.21	305.29	9.54
2004–2011	84.39	12.06	667.46	95.35	1972–2011	1170.38	30.01	388.10	9.95
2011–2017	910.04	151.67	12.04	2.01	1972–2017	1943.34	43.19	263.07	5.85
2017–2021	719.28	179.82	1.37	44.95	1972–2021	2582.77	52.71	184.60	3.77
Average		90.08		25.05			62.92		7.68

Fig. 4 Short-term erosion–accretion in Sagar island (**a** and **b**) and long-term erosion–accretion in Sagar island (**c** and **d**) (1:320,000 scale) during the different time periods from 1972 to 2021

of these channels (Dubey et al., 2014; Maheshvaran et al., 2019; Saichenthur et al., 2021). This may be one of the reasons that the western side gets eroded enormously.

Ghoramara island

Ghoramara island, which is located near the entrance of the Muriganga River, is reduced to less than half of its area from 916.78 ha (1972) to 355.77 ha (2021) within the last five decades (1972–2021) (Fig. 2c). The short-term and long-term average erosion is found as 11.85 ha/year and 13.63 ha/year, respectively. However, the accretion rates are comparatively negligible which are 0.85 ha/year and 0.15 ha/year in the short- and long-term, respectively (Table 4). The erosion takes place continuously around all sides

(Fig. 5) without keeping the shape unchanged. This is probably due to the reason that the Hooghly river directly hits the northern side, the tidal impact hits the southern side, and the bifurcated flow erodes the eastern and western side.

Basit island

Basit island is located at the upper most region of the Muriganga River. This island has expanded enormously from 1972 till now (Fig. 2g). The average rate of accretion for short-term and long-term are found as 16.62 ha/year and 279.97 ha/year, respectively (Table 5). The accretion takes place from all sides (Fig. 6a, c). The initial area of this island in 1972 was 18.65 ha, whereas in 2021, the area became 647.47 ha. Most of the accretion is found in the period of

Table 4 Short-term and long-term erosion accretion rate in Ghoramara island

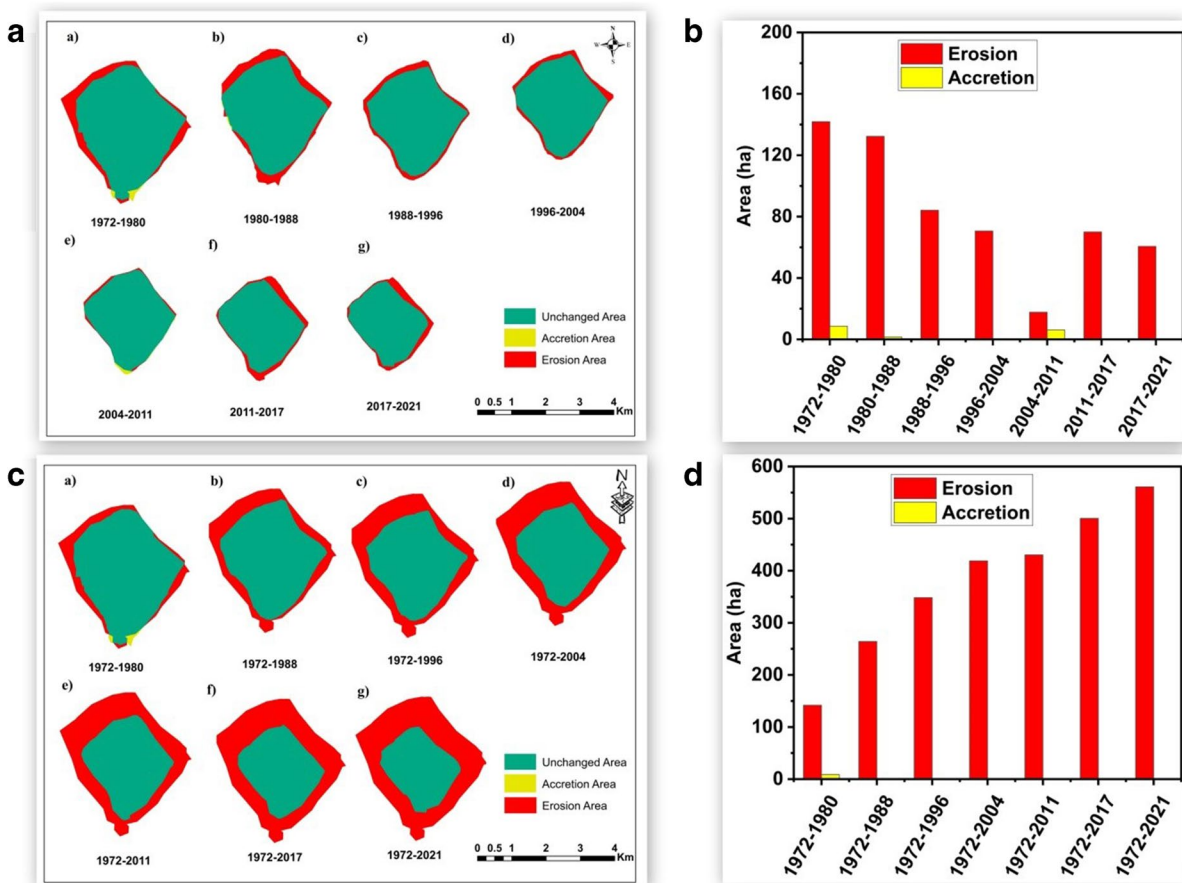| Short-term erosion accretion rate					Long-term erosion accretion rate				
Duration	Erosion		Accretion		Duration	Erosion		Accretion	
	Total (ha)	Rate (ha/y)	Total (ha)	Rate (ha/y)		Total (ha)	Rate (ha/y)	Total (ha)	Rate (ha/y)
1972–1980	141.89	17.74	8.58	2.22	1972–1980	141.89	17.74	8.58	1.07
1980–1988	132.31	16.54	1.58	2.07	1972–1988	264.05	16.50	0.00	0.00
1988–1996	84.16	10.52	0.00	1.31	1972–1996	348.21	14.51	0.00	0.00
1996–2004	70.64	8.83	0.00	0.00	1972–2004	418.85	13.09	0.00	0.00
2004–2011	17.72	2.53	6.15	0.36	1972–2011	430.42	11.04	0.00	0.00
2011–2017	69.99	11.66	0.00	0.00	1972–2017	500.41	11.12	0.00	0.00
2017–2021	60.61	15.15	0.00	0.00	1972–2021	561.01	11.45	0.00	0.00
Average		11.85		0.85			13.63		0.15

Fig. 5 Short-term erosion–accretion in Ghoramara island (a and b) and long-term erosion–accretion in Ghoramara island (c and d) (1:60,000 scale) during different time periods from 1972 to 2021

Table 5 Short-term and long-term erosion accretion rate in Basit island

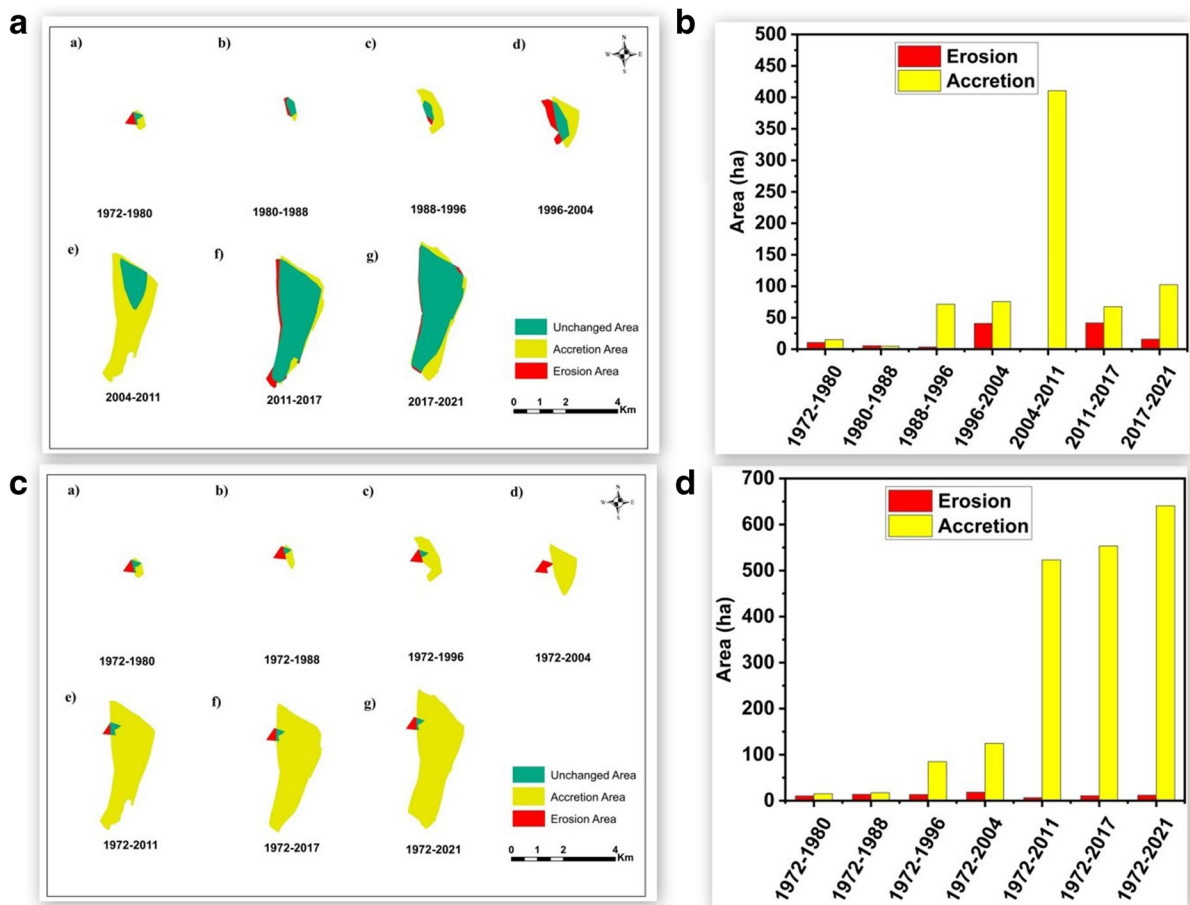| Short-term erosion accretion rate					Long-term erosion accretion rate				
Duration	Erosion		Accretion		Duration	Erosion		Accretion	
	Total (ha)	Rate (ha/y)	Total (ha)	Rate (ha/y)		Total (ha)	Rate (ha/y)	Total (ha)	Rate (ha/y)
1972–1980	10.57	1.32	15.19	1.90	1972–1980	10.57	1.32	55.72	15.19
1980–1988	5.54	0.69	4.66	0.58	1972–1988	13.78	0.86	127.09	17.51
1988–1996	3.55	0.44	71.35	8.92	1972–1996	13.37	0.56	162.01	84.90
1996–2004	41.01	5.13	75.53	9.44	1972–2004	18.55	0.58	207.45	124.61
2004–2011	0.11	0.02	410.63	58.66	1972–2011	6.71	0.17	216.99	523.29
2011–2017	41.72	6.95	67.58	11.26	1972–2017	10.95	0.24	223.57	553.40
2017–2021	15.92	3.98	102.30	25.58	1972–2021	12.08	0.25	225.32	640.90
Average		2.65		16.62			0.57		279.97

Fig. 6 Short-term erosion–accretion in Basit island (a and b) and long-term erosion–accretion in Basit island (c and d) (1:80,000 scale) during the different time periods from 1972 to 2021
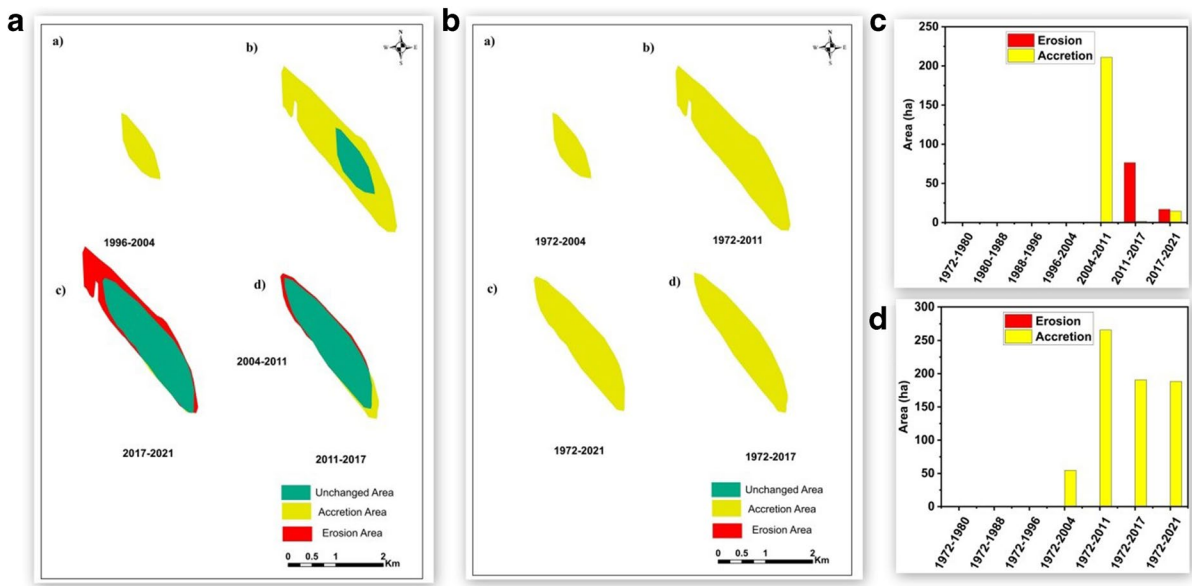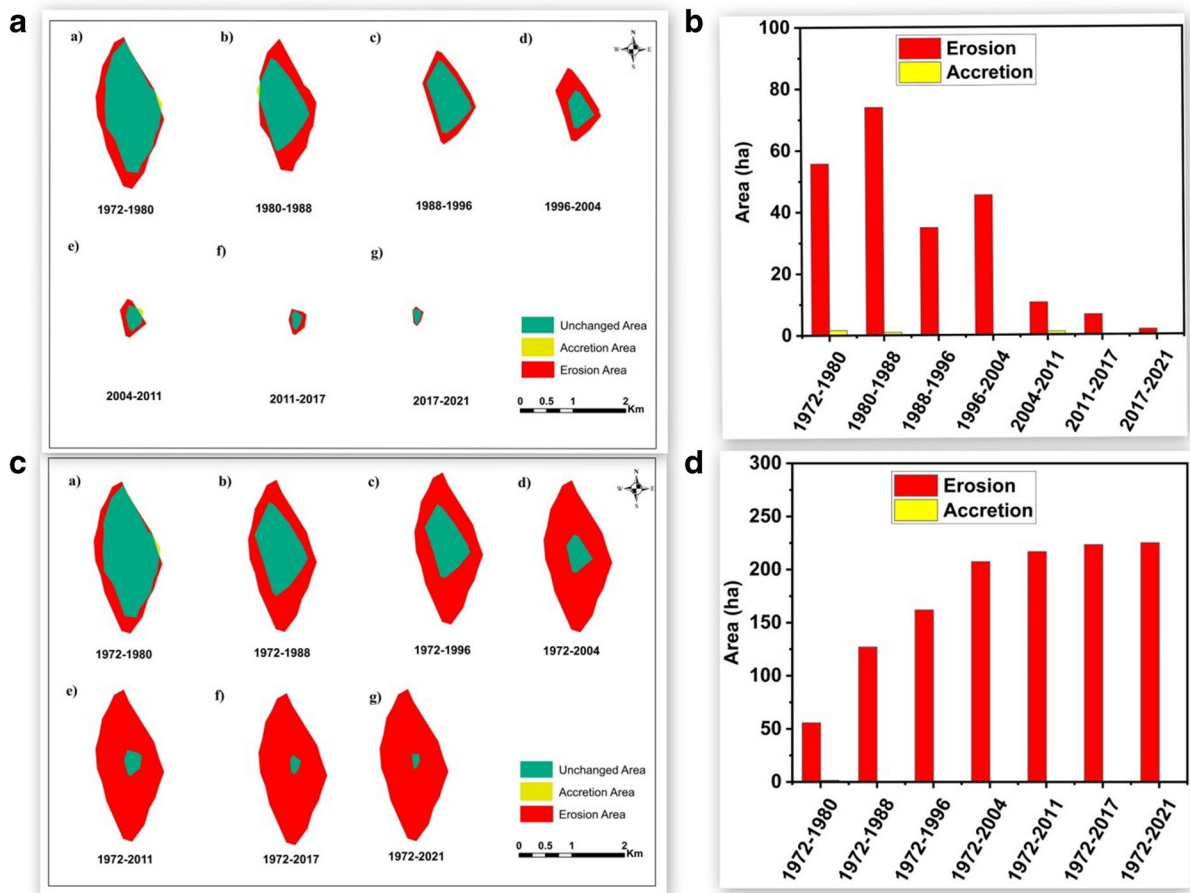
Fig. 7 Short-term erosion–accretion in Niogi island (a and b) and long-term erosion–accretion in Niogi island (c and d) (1:40,000 scale) during the different time periods from 1972 to 2021

2004–2011. Probably, the flow gets reduced while hitting the northern side of the island, and the upstream eroded materials get deposited at the tail of it.

Niogi island

With the help of the multi-temporal Landsat images, it is found that the Niogi island has emerged in 2004 onwards (Fig. 7). Before that, this island may be in submerged condition. The island becomes visible due to the gradual depositions over the years. This newly developed island had an area of 50.64 ha in 2004, and

it has become 188.34 ha in 2021 (Fig. 2h). The average accretion rates in short-term and long-term analysis are very less compared to erosion (Table 6). This island is continuously expanding year after year.

Pushpa island

The Pushpa island is on the way to extinction because of continuous erosion. The average rates of short-term and long-term erosion are found as 4.19 ha/year and 6.18 ha/year, and the accretion rates are 0.07 ha/year and 0.23 ha/year (Table 7). This has

Table 6 Short-term and long-term erosion accretion rate in Niogi island

Short-term erosion accretion rate					Long-term erosion accretion rate				
Duration	Erosion		Accretion		Duration	Erosion		Accretion	
	Total (ha)	Rate (ha/y)	Total (ha)	Rate (ha/y)		Total (ha)	Rate (ha/y)	Total (ha)	Rate (ha/y)
1972–1980	0.00	0.00	0.00	0.00	1972–1980	0.00	0.00	0.00	0.00
1980–1988	0.00	0.00	0.00	0.00	1972–1988	0.00	0.00	0.00	0.00
1988–1996	0.00	0.00	0.00	0.00	1972–1996	0.00	0.00	0.00	0.00
1996–2004	0.00	0.00	0.00	0.00	1972–2004	0.00	0.00	54.64	1.71
2004–2011	0.00	0.00	211.05	30.15	1972–2011	0.00	0.00	265.69	6.81
2011–2017	76.46	12.74	1.52	0.25	1972–2017	0.00	0.00	190.75	4.24
2017–2021	16.89	4.22	14.48	3.62	1972–2021	0.00	0.00	188.34	3.84
Average		2.42		4.86			0.00		2.37

Table 7 Short-term and long-term erosion accretion rate in Pushpa island

Short-term erosion accretion rate					Long-term erosion accretion rate				
Duration	Erosion		Accretion		Duration	Erosion		Accretion	
	Total (ha)	Rate (ha/y)	Total (ha)	Rate (ha/y)		Total (ha)	Rate (ha/y)	Total (ha)	Rate (ha/y)
1972–1980	55.72	6.96	1.64	0.21	1972–1980	55.72	6.96	55.72	1.64
1980–1988	74.03	9.25	1.02	0.13	1972–1988	127.09	7.94	127.09	0.00
1988–1996	34.91	4.36	0.00	0.00	1972–1996	162.01	6.75	162.01	0.00
1996–2004	45.44	5.68	0.00	0.00	1972–2004	207.45	6.48	207.45	0.00
2004–2011	10.57	1.51	1.04	0.15	1972–2011	216.99	5.56	216.99	0.00
2011–2017	6.58	1.10	0.00	0.00	1972–2017	223.57	4.97	223.57	0.00
2017–2021	1.76	0.44	0.01	0.00	1972–2021	225.32	4.60	225.32	0.00
Average		4.19		0.07			6.18		0.23

Fig. 8 Short-term erosion–accretion in Pushpa island (a and b) and long-term erosion–accretion in Pushpa island (c and d) (1:40,000 scale) during the different time periods from 1972 to 2021

lost almost 98% of its area from 228.56 ha (1972) to 3.24 ha (2021) (Fig. 2f). The erosion takes place from all sides (Fig. 8), and it is probably going to disappear in the upcoming days.
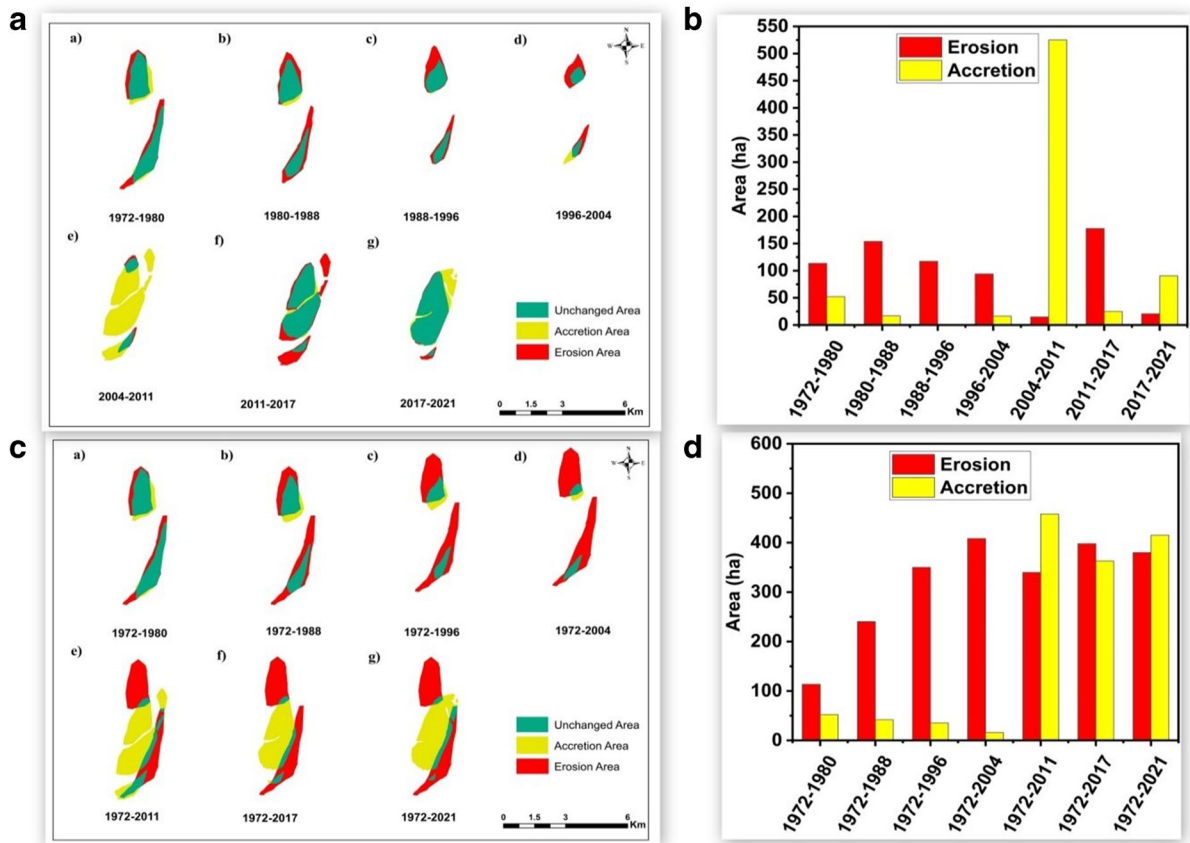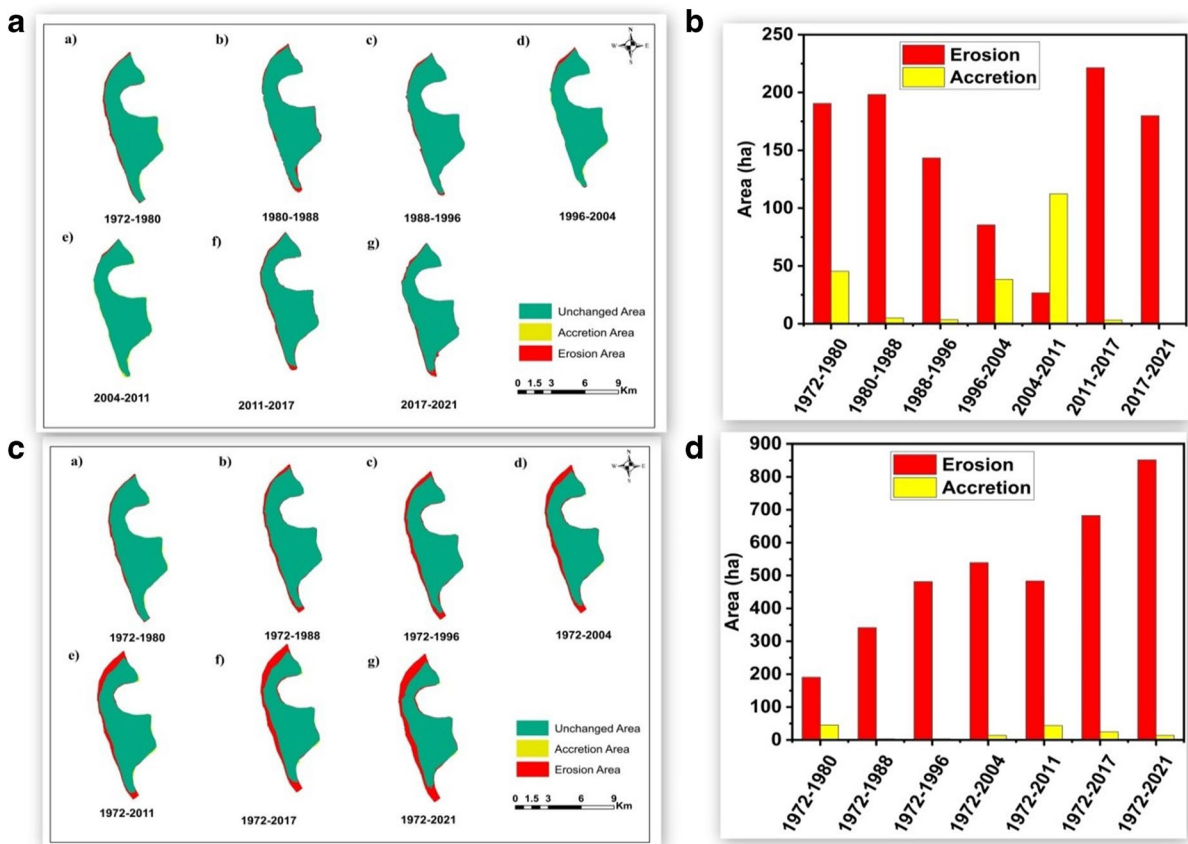
Fig. 9 Short-term erosion–accretion in Half-fish island (a and b) and long-term erosion–accretion in Half-fish island (c and d) (1:100,000 scale) during the different time periods from 1972 to 2021

Half-fish island

The Half-fish island is one of the most dynamic island in the Muriganga River. The land started shrinking till 2004. The land gradually reduced to about 1/6th of its original area in 2004 (Fig. 2e). There is an abrupt amount of accretion that took place in 2011 (Fig. 9a, b). The average

Table 8 Short-term and long-term erosion accretion rate in Half-fish island

Short-term erosion accretion rate					Long-term erosion accretion rate				
Duration	Erosion		Accretion		Duration	Erosion		Accretion	
	Total (ha)	Rate (ha/y)	Total (ha)	Rate (ha/y)		Total (ha)	Rate (ha/y)	Total (ha)	Rate (ha/y)
1972–1980	113.54	14.19	52.24	6.53	1972–1980	113.54	14.19	52.24	6.53
1980–1988	153.91	19.24	16.72	2.09	1972–1988	240.34	15.02	41.84	2.61
1988–1996	117.24	14.65	1.05	0.13	1972–1996	349.89	14.58	35.21	1.47
1996–2004	93.91	11.74	16.27	2.03	1972–2004	408.28	12.76	15.96	0.50
2004–2011	14.79	2.11	525.06	75.01	1972–2011	339.84	8.71	457.78	11.74
2011–2017	177.81	29.64	25.06	4.18	1972–2017	397.79	8.84	362.98	8.07
2017–2021	20.51	5.13	90.45	22.61	1972–2021	379.91	7.75	415.04	8.47
Average		13.81		16.08			11.69		5.63

Table 9 Short-term and long-term erosion accretion rate in Mousuni island

Short-term erosion accretion rate					Long-term erosion accretion rate				
Duration	Erosion		Accretion		Duration	Erosion		Accretion	
	Total (ha)	Rate (ha/y)	Total (ha)	Rate (ha/y)		Total (ha)	Rate (ha/y)	Total (ha)	Rate (ha/y)
1972–1980	190.54	23.82	45.36	5.67	1972–1980	190.54	23.82	45.36	5.67
1980–1988	198.28	24.78	4.98	0.62	1972–1988	341.42	21.34	2.95	0.18
1988–1996	143.38	17.92	3.52	0.44	1972–1996	481.48	20.06	3.14	0.13
1996–2004	85.55	10.69	38.44	4.81	1972–2004	539.07	16.85	13.62	0.43
2004–2011	26.73	3.82	112.30	16.04	1972–2011	483.58	12.40	43.70	1.12
2011–2017	221.41	36.90	3.26	0.54	1972–2017	682.36	15.16	24.33	0.54
2017–2021	179.94	44.98	0.11	0.03	1972–2021	851.71	17.38	13.85	0.28
Average		23.27		4.02			18.14		1.19

short-term and long-term erosion rates are 13.81 ha/year and 11.69 ha/year (Table 8). The land expanded from 2011 onward, and the area is found as 507.05 ha in 2021.

Mousuni island

Mousuni island is located in the downmost region of the Muriganga River. This island is famous as a

Fig. 10 Short-term erosion–accretion in Mousuni island (a and b) and long-term erosion–accretion in Mousuni island (c and d) (1:190,000 scale) during the different time periods from 1972 to 2021

tourist place. In Mousuni island, the short-term and long-term average erosion and accretion rates are 23.27 ha/year and 18.14 ha/year and 4.02 ha/year and 1.19 ha/year, respectively (Table 9). From short-term analysis, it is found that between the 2004 and 2011 period, the accretion is relatively greater than the erosion (Fig. 10a, b) on the southern side. From Fig. 10, it is clear that the main concern is the western side, which undergoes severe erosion.

Spatio-temporal shoreline changes analysis using DSAS

Both the left and the right banks are divided into three sectors each. The three sectors of the left bank are Kakdwip, Namkhana and Rajnagar (Fig. 11), whereas the three sectors of right bank are Kachuberia, Kaylapara and Chemaguri (Fig. 12). Based on LRR and EPR, both the left and the right bank are classified into seven categories as shown in Table 10.

Based on the EPR values, the maximum rate of erosion for left bank is 23.91 m/year at the Rajnagar sector near Fraserganj. Here, the LRR shows the erosion of 13.76 m/year. The maximum erosion based on LRR is 14.25 m/year at the Namkhana sector near Nadabhanga, where the EPR shows an erosion rate of 14.58 m/year. The maximum accretion rate for the left bank based on EPR is 5.18 m/year at the Rajnagar sector near Janamore, where the LRR also gives the maximum value of 6.75 m/year. The maximum erosion based on NSM is about 1170 m at the Rajnagar sector near Fraseganj, whereas the maximum accretion is about 253 m at the Rajnagar sector near Janamore. The overall average erosion throughout the entire left bank based on EPR, LRR and NSM are 7.31 m/year, 6.67 m/year and 358.57 m. Furthermore, the overall accretions are found as 1.19 m/year, 1.48 m/year and 58.24 m based on EPR, LRR and NSM, respectively. The erosion–accretion profile throughout the entire left and right bank is shown in Fig. 13 and
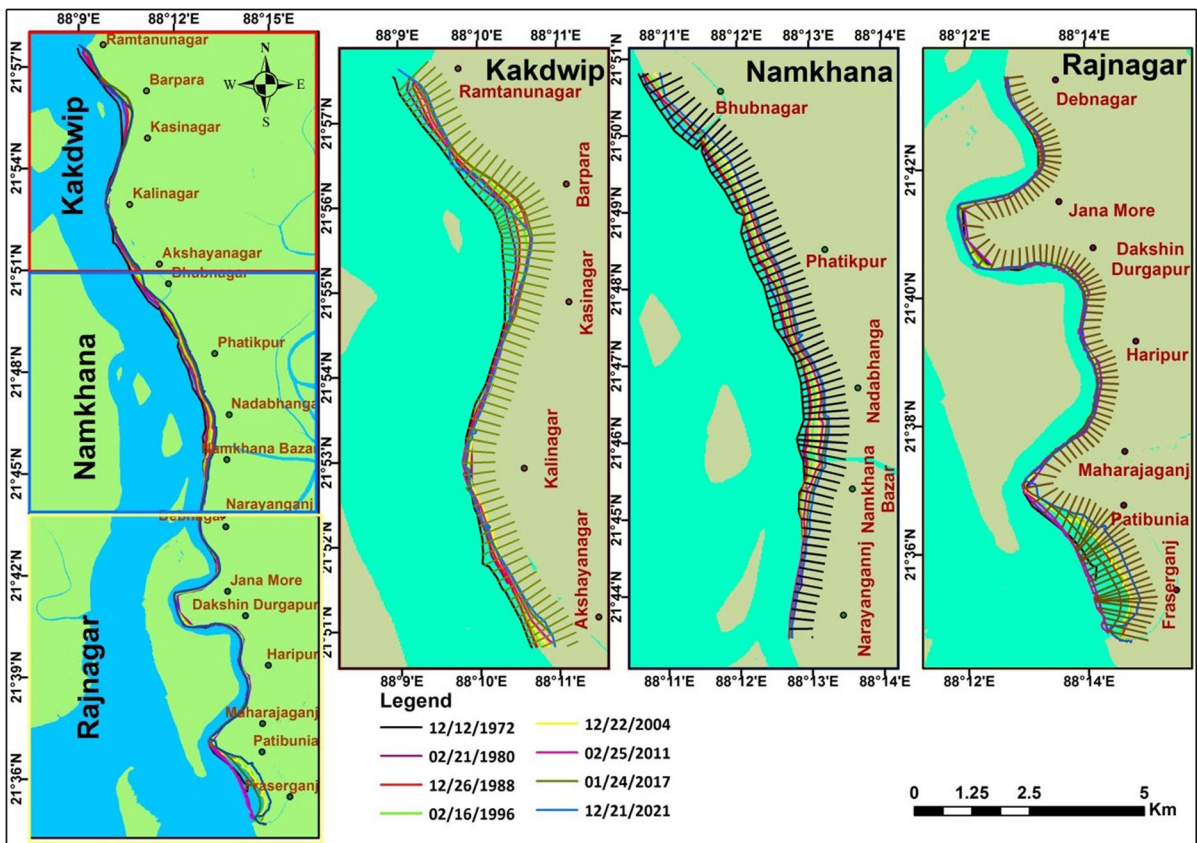

Fig. 11 Location map of different sectors of the left bank of the Muriganga River
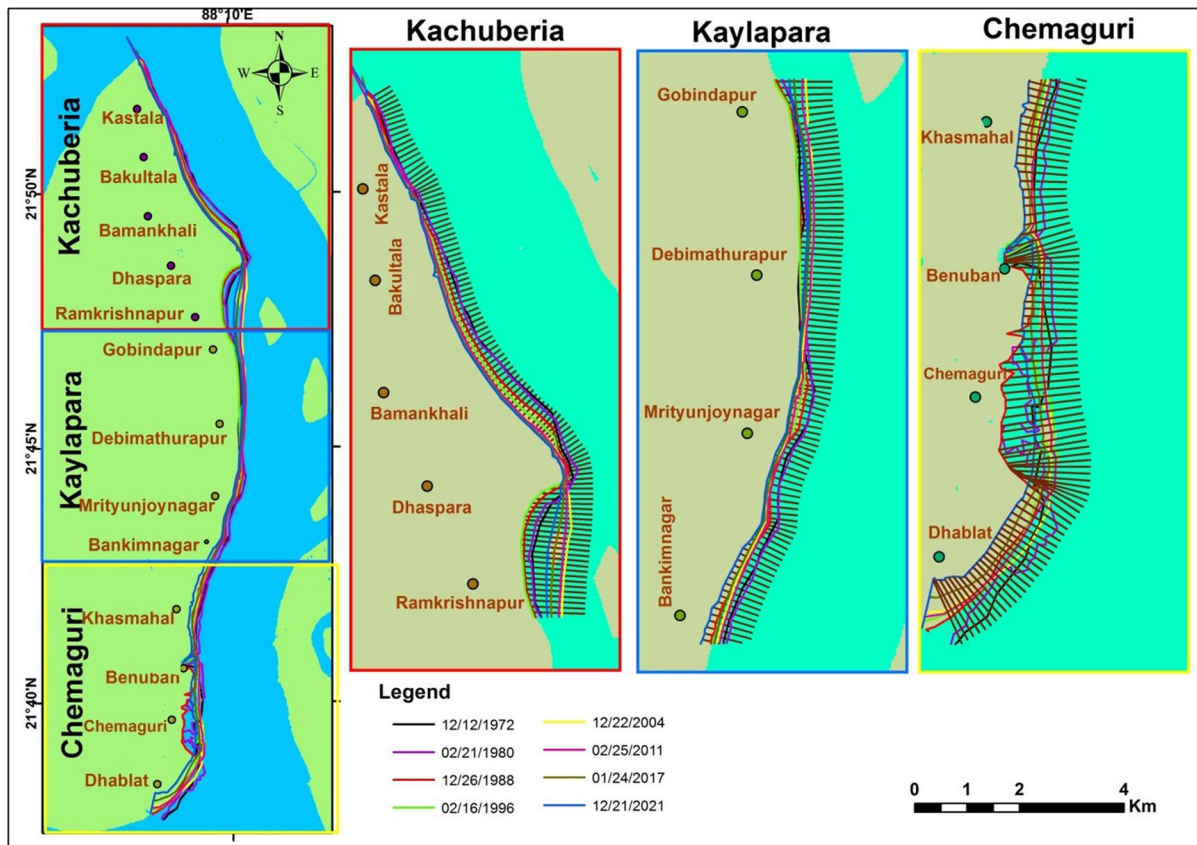
Fig. 12 Location map of different sectors of the right bank of the Muriganga River

Fig. 14, respectively, which takes place from 1972 to 2021. The maximum erosion rates at the right bank are 19.28 m/year (EPR) and 15.96 (LRR) at the lowermost region of the Chemaguri sector near Dhablat.

Table 10 Shoreline classifications based on erosion (negative values) and accretion (positive values) rates calculated from EPR and LRR

Sl No.	Classifications	Rate of shore-line change (m/y)
1	Very high erosion	< −6
2	High erosion	≥ −6 and < −3
3	Moderate erosion	≥ −3 and ≤ 0
4	Stable	0
5	Moderate accretion	> 0 and ≤ 3
6	High accretion	> 3 and ≤ 6
7	Very high accretion	> 6

The maximum accretion rate is found as 13.01 m/year (LRR) at the Kachuberia sector near Ramkrishnapur.

Chemaguri sector The maximum erosion rates are 19.28 m/year (EPR) and 15.96 (LRR) at the lowermost region of this sector near Dhablat (Fig. 15). However, the maximum accretion rates are found as 8.63 m/year (EPR) and 12.14 m/year (LRR) near Benuban. Near Benuban region, very high accretion is found, whereas moderate accretion is found in the upper half between Dhablat and Chemaguri. The rest of the entire sector is showing high to very high erosion. Dhablat, lower region of Benuban, and Khasmahal are under severe condition. They are losing their lands day by day.

Kaylapara sector The maximum erosion rates are 7.48 m/year (EPR) and 7.40 (LRR) near Mrityunjoynagar (Fig. 16). The maximum accretion rates are found as 2.38 m/year (EPR) and 6.15 m/year (LRR)

Fig. 13 Erosion–accretion profile at different sectors in the left bank of the Muriganga River calculated using EPR (a), LRR (b) and NSM (c) during the period of 1972 to 2021
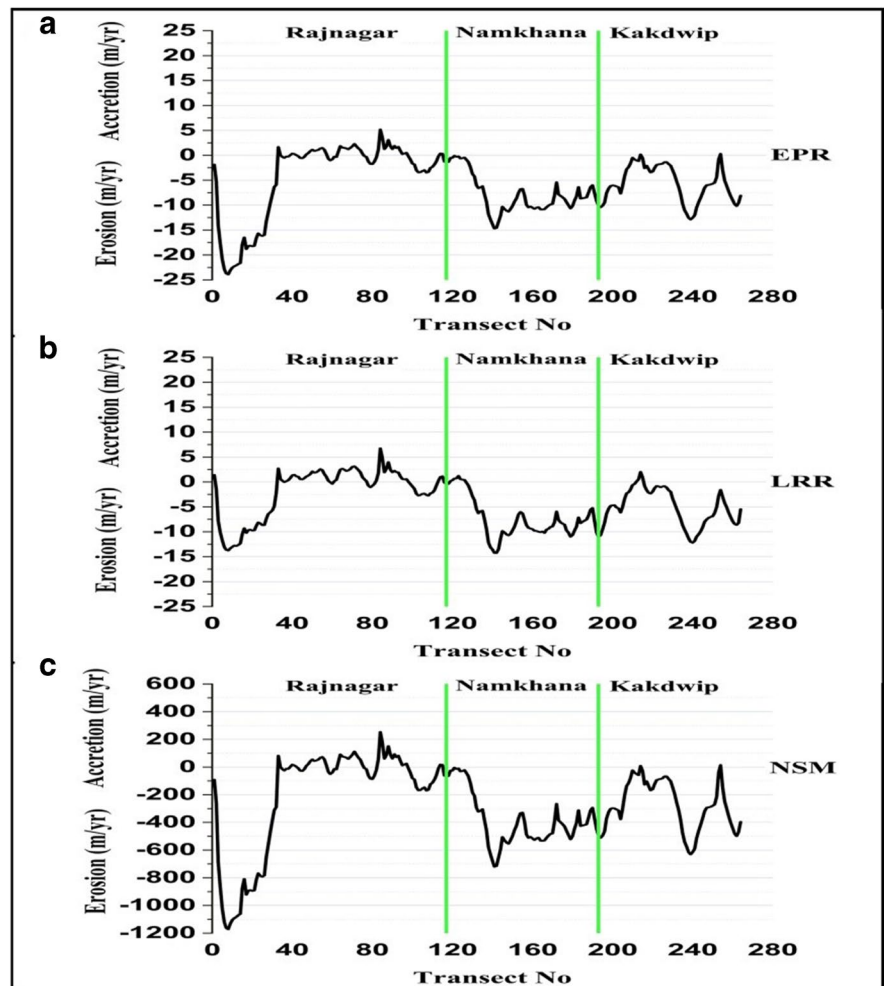

at the topmost transect of this sector near Gobindapur. Between Gobindapur and Debimathurapur, a moderate accretion is found. This is possibly due to the deposition of the erosive materials of Pushpa island. In between Mrityunjoynagar to Bankimnagar, a high to very high erosion can be seen. The probable reason behind it may be the tidal and cyclonic activities, waves, land subsidence etc. Mrityunjoynagar and Bankimnagar are under the area of consideration because the land is shrinking due to high erosion.

Kachuberia sector Above Dhaspara to the topmost region of the sector is showing high to very high erosion (Fig. 17). The maximum erosion rates are 9.90 m/year (EPR) and 10.46 (LRR) near Bamankhali. The maximum accretion rates are found as 5.97 m/year (EPR) and 13.01 m/year (LRR) near

Ramkrishnapur. Moderate to high and high to very high erosion zones are found near Kastala. The erosion at Kastala, Bakultala, Bamankhali and Dhaspara may be due to the change in complex hydrodynamics in the estuarine region. The banks in Ramkrishnapur may be in a submerged condition, which leads to accretion in that area due to low water depth.

Rajnagar sector The maximum erosion rates are 23.91 m/year (EPR) and 13.76 (LRR) near Fraserganj (Fig. 18). The maximum accretion rates are found as 5.18 m/year (EPR) and 6.75 m/year (LRR) near Janamore. Both erosion and accretion are found in this sector. From Maharajaganj to Debnagar, moderate erosion to moderate accretion is found. The lower one-third shows high to very high erosion. This is may be due to the meandering pattern of the river and

Fig. 14 Erosion–accretion profile at different sectors in the right bank of the Muriganga River calculated using EPR (a), LRR (b) and NSM (c) during the period of 1972 to 2021
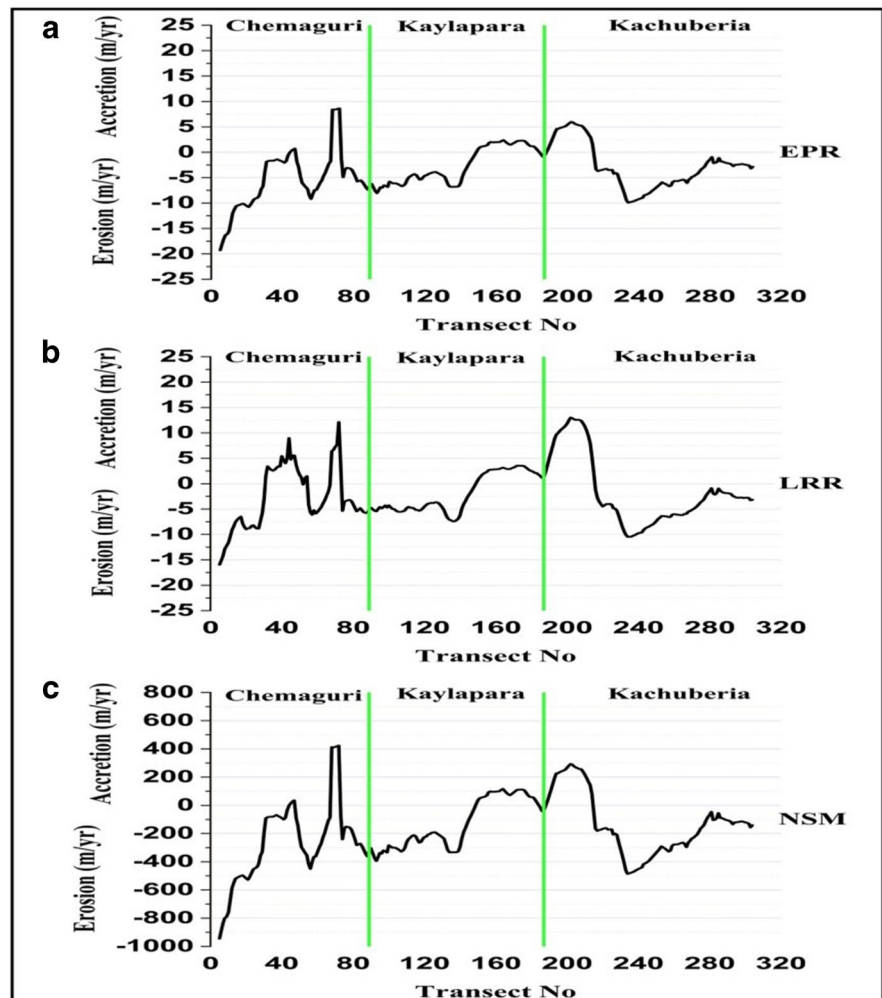
the tidal impact. The Patibunia and Fraserganj are experiencing high to very high erosion. Fraserganj is experiencing erosion, possibly due to the high tidal force and sea-level rise, as it is situated in the seaward region.

Namkhana sector This sector is mainly dominated by erosion. The maximum erosion rates are 14.58 m/year (EPR) and 14.25 (LRR) near Nadabhanga, whereas the maximum accretion rates are 0.8 m/year (EPR) and 1.22 m/year (LRR) near Narayanganj. Fig. 19 clearly depicts that the entire sector is almost erosive in nature. The average values of EPR, LRR and NSM are −7.82 m/year (i.e. erosion), −7.37 m/year (i.e. erosion) and −383.54 m (erosion), respectively. Almost the entire sector is under severe threat. The probable reason may be the landslide, the

curvature of the river and furthermore the man-made activity.

Kakdwip sector This sector is also mainly dominated by erosion. The maximum erosion rates are 12.88 m/year (EPR) and 12.20 (LRR), whereas the maximum accretion rates are 0.30 m/year (EPR) and 2.03 m/year (LRR) (Fig. 20). The average values of EPR, LRR and NSM are −5.67 m/year (i.e. erosion), −5.24 m/year (i.e. erosion) and −278.46 m (erosion), respectively. Ramtanunagar, Barpara and Akshaynagar are in the zone of very high erosion, while Kalinagar is in moderate erosion zone. The entire sector is facing severe erosion, possibly due to the curvature of the river, tidal impact and some man-made activities like deforestation, excavations and improper urbanization.
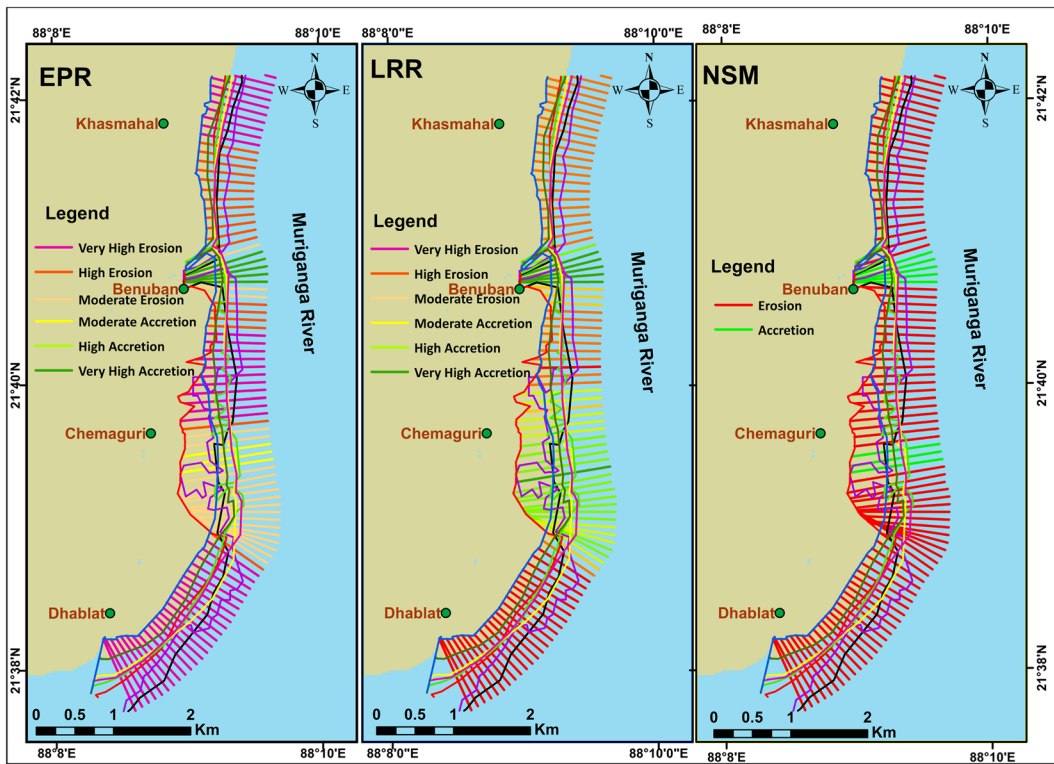
Fig. 15 Assessments of different degrees of erosion–accretion in the Chemaguri sector during the time period of 1972 to 2021 from EPR, LRR and NSM

Discussion

The changes in the Muriganga River and in the islands are analysed in this study. The shoreline is considered as one of the most dynamic features on the earth's surface (Adarsa et al., 2012; Bandyopadhyay et al., 2004; Chakraborty, 2013; Laha & Bandyapadhyay, 2013). The coastal shoreline changes occurred due to the complex interaction between regional forcing factors such as tidal effect (Gratiot et al., 2008), sea-level rise (Zhang et al., 2004), meandering pattern (Van De Wiel, 2003), magnitude of wave energy, morphological properties, sediment supply and sediment budget (Amin & Davidson-Arnott, 1997). Moreover, the dredging activity is also an important factor responsible for comparatively faster changes in shoreline position (Demir et al., 2004; Jones et al., 2016; Monge-Ganuzas et al., 2013; Morris, 2007).

The Hooghly estuarine system is known as one of the most complex estuary in the world (Bakshi & Bhar, 2020). Flat sandy beaches, mud flats, tidal marsh etc. are found on the bank of the Muriganga River. Tidal flats are found within high tide and low tidal zones around the open shore. Silty sand and hard muddy patches are found in the high tidal flats. Mostly, silts and clay are found in the low tidal flats (Fig. 21). The left bank of the Muriganga River consists of three sectors Rajnagar, Namkhana and Kakdwip. The right bank is nothing but the eastern side of Sagar island. This bank consists of three sectors Chemaguri, Kaylapara and Kachuberia sectors. The southwestern, southern and southeastern region of Sagar island mainly consists of sand where sand content is more than 80% (Nandi et al., 2016). These sandy beaches are highly erodible by the forces like wind, wave and tidal impacts.

Analysis of shoreline migration

The shoreline changes in the Muriganga River and the islands are calculated with the help of remote sensing and GIS techniques and the DSAS tool by using
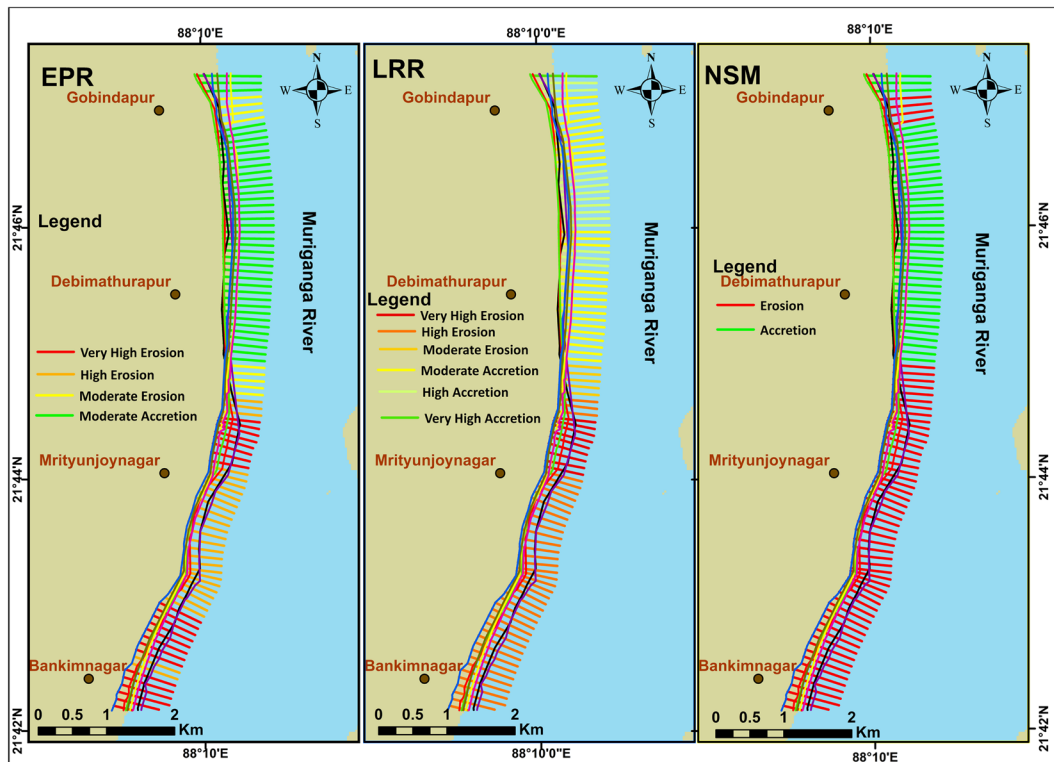
Fig. 16 Assessments of different degrees of erosion–accretion in the Kaylapara sector during the time period of 1972 to 2021 from EPR, LRR and NSM

the multi-temporal Landsat data. One of the factors which influence the erosion–accretion process is the meandering in the river. Generally, the concave site shows least erosion (more accretion), and the convex site shows least accretion (more erosion). The velocity is higher in convex bank and lower in the concave bank. Therefore, the shear stress is higher in the convex site compared to the concave site. Moreover, the helical flow directs water and sediment toward the concave bank and away from the convex bank which leads to the accumulation of sediments on the concave side. Fig. 1 clearly depicts that the outer side of the left bank of Muriganga River is convex and that the right bank is concave. From DSAS analysis, it is clear that both the banks are getting eroded by an average rate of 5.73 m/year (EPR) and 4.35 m/year (LRR) for the left bank and 3.48 m/year (EPR) and 2.06 m/year (LRR) for the right bank. The higher erosion is found on the left bank (Fig. 22). The overall area of the Muriganga River has increased by 16.82 % from 14,029.42 ha in 1972 to 16,390.02 ha in 2021,

which indicates that overall, the Muriganga River is of degrading type. Another study by Dutta et al. (2022) also found that the erosion rate in the left bank at Kakdwip and Namkhana is >5 m/year. From the analysis, it can be said that the eroded materials of the bank are deposited in few downstream islands like Basit and Niogi.

From DSAS analysis, the maximum erosion rate based on EPR and LRR is 23.91 m/year and 13.76 m/year for the left bank, which occurs at the lower side of the Rajnagar sector near Fraserganj. This place is situated at the most downstream region on the left bank. It is very obvious here that the tides are very much prominent which hits the bank with great impact. The maximum accretion rates on the left bank are found as 5.18 m/year (EPR) and 6.75 m/year (LRR) at the Rajnagar sector in between Janamore and Dakshin Durgapur. Here, the concave shape of the shoreline is probably responsible for the accretion. The maximum erosion rate for the right bank is found at as 19.28 m/year (EPR) and 15.96 (LRR)
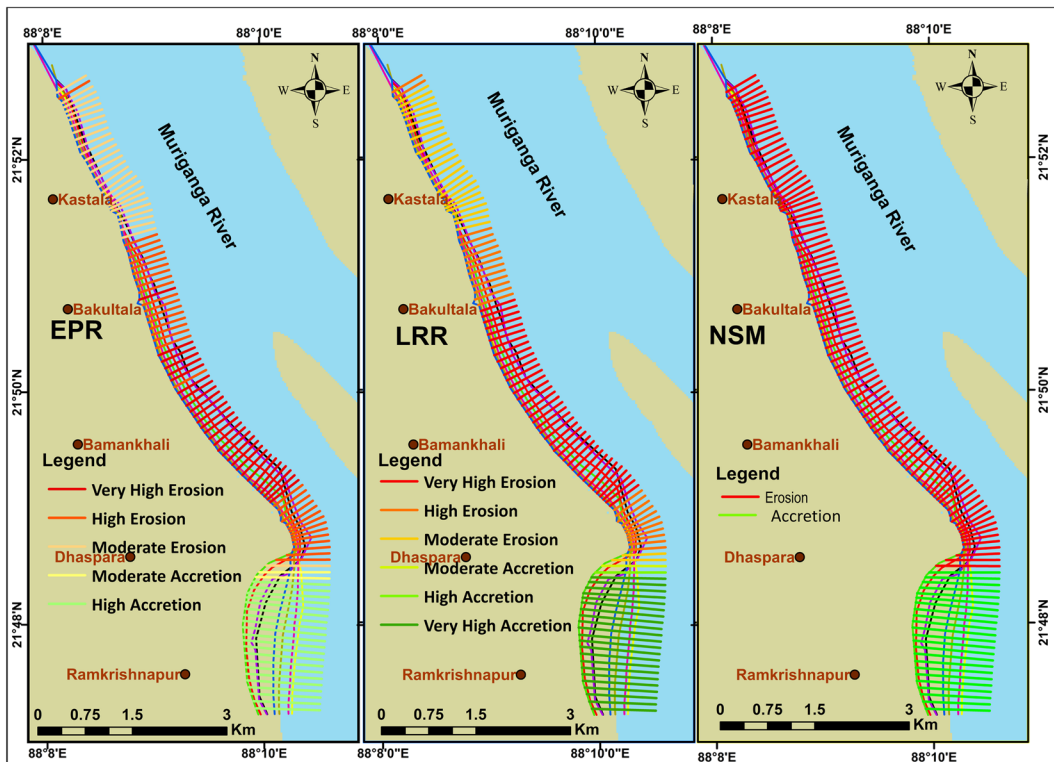
Fig. 17 Assessments of different degrees of erosion–accretion in the Kachuberia sector during the time period of 1972 to 2021 from EPR, LRR and NSM

at the bottom at the Chemaguri sector near Dhablat. The lower most region of the right bank which is nothing but the eastern side of Sagar island is facing tidal and cyclonic activity, sea-level rise and waves as stated earlier. The maximum accretion rates on the right bank are found as 5.97 m/year (EPR) and 13.01 m/year (LRR) at the Kachubeia sector near Ramkrishnapur. The heavy, curvy shape of the Dhaspara region, which is just above the Ramkrishnapur, may reduce the flow velocity. Therefore, the sediment may not cross its settling velocity, which further leads to accretion in this location.

Overall, high to very high erosion is found at Chemaguri sector. Mainly, Dhablat, lower region of Benuban, Khasmahal, is under severe condition (Fig. 15). This sector is located at the downmost side of the right bank. The tidal influence is higher in that region, which leads in eroding the bank material. In the Kaylapara sector, the upper region shows some accretion, while the lower part shows erosion. High to very high erosion is found near Mrityunjoynagar

and Bankimnagar (Fig. 16). In the Kachuberia sector, the maximum erosion is found near Bamankhali (Fig. 17). The overall convex shape of the left bank shows significant erosion at an average rate of 5.73 m/year (EPR) and 4.35 m/year (LRR). The tidally influenced Fraserganj in the Rajnagar sector shows maximum erosion (Fig. 18). The meandering shape of this region shows both erosion and accretion. Almost the entire Namkhana sector shows a high rate of erosion. Namkhana Bazar, Nadabhanga, Phatikpur and Bhubnagar are such highly erosive places (Fig. 19). In the Kakdwip sector, high to very high erosion is found near Ramtanunagar, Barpara and Akshaynagar, while Kalinagar is under moderate erosion zone (Fig. 20).

Field visit at Kakdwip sector reveals that the tidal influence is not much prominent at this sector. Due to its convex shape, the upstream flow directly hits the bank and creates substantial shear force which is one of the significant factors of bank erosion (Fig. 22).

Mainly due to fluvial action, the cliff erosion is also very prominent in these locations. Localized
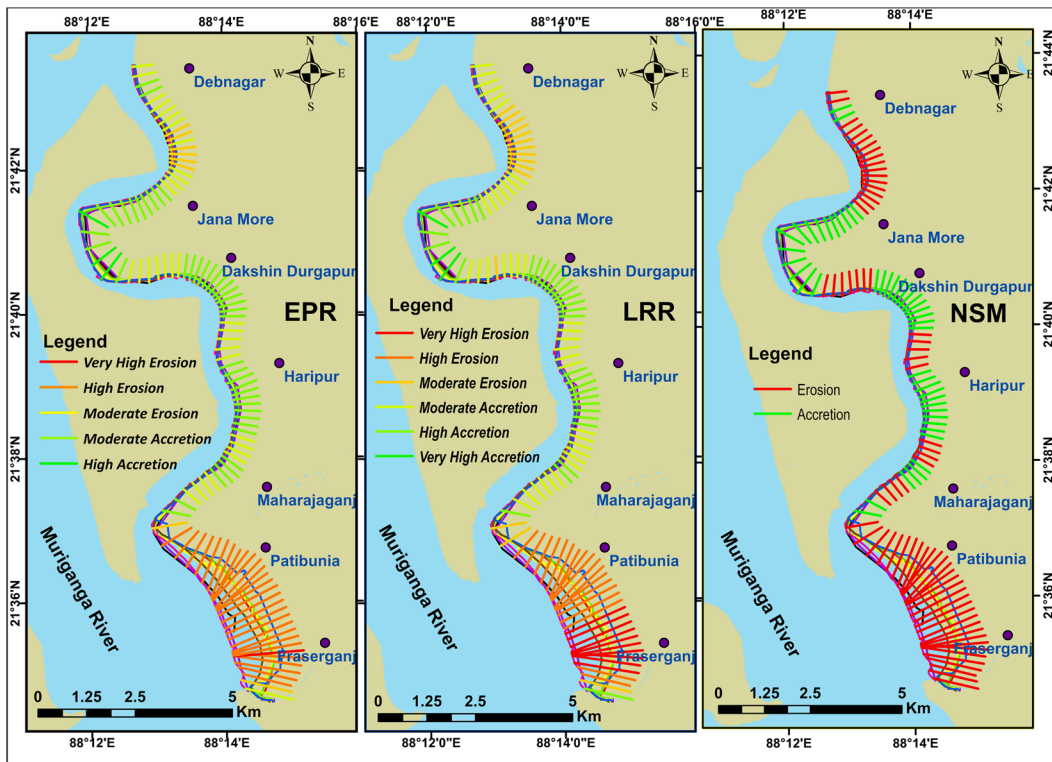
Fig. 18 Assessments of different degrees of erosion–accretion in the Rajnagar sector during the time period of 1972 to 2021 from EPR, LRR and NSM

mud decoupling at the toe on the left bank is seen near Akshyanagar (Fig. 23).

In order to reduce the erosion, the local authorities have constructed wooden embankment along the river bank in the vulnerable locations (Fig. 24). These structures ultimately reduced the total erosion in these areas, and that is why these zones are of moderate erosion zone. These types of coastal management plans are required in areas where currently high erosion rate is observed (e.g. Fraserganj, Patibunia, entire Namkhana sector).

Analysis of island dynamics

From the long-term analysis, it is found that the erosion and accretion rates for Sagar island are 62.92 ha/year and 7.68 ha/year (Table 3). Almost 50% of the area of Ghoramara island is eroded at a rate of 13.63 ha/year (Table 4) from all sides by keeping its shape unchanged (Fig. 5). Similarly, Pushpa island has lost almost 98% of its area at a rate of 6.18 ha/

year (Table 7) from all the sides (Fig. 8). It may disappear in upcoming years. Basit (Fig. 6) and Niogi (Fig. 7) islands are getting accreted, probably due to the deposition of the sediments carried out by the upstream Hooghly river and the eroded bank materials of the left bank of the Muriganga River. The Mousuni island located at the downstream region of the Muriganga River is continuously eroding at 18.14 ha/year (Table 9). Mainly, the western side of this island is subjected to erosion (Fig. 10), probably due to the combined effects of rising sea levels, rising wave form velocity, tidal impacts, cyclonic activity etc.

Increase in sea level can lead the storm surge and wave to move further inland. The rising sea level, violent cyclones, coastal erosion etc. are found near Sagar island due to the change in climate conditions (Bera et al., 2022). The relative mean sea-level rise at 3.14 mm/year was found near Sagar island (Hazra et al., 2002). From the observed data between 2002 and 2009, the apparent sea-level rise in Sagar and Sundarban regions are varying within the range of
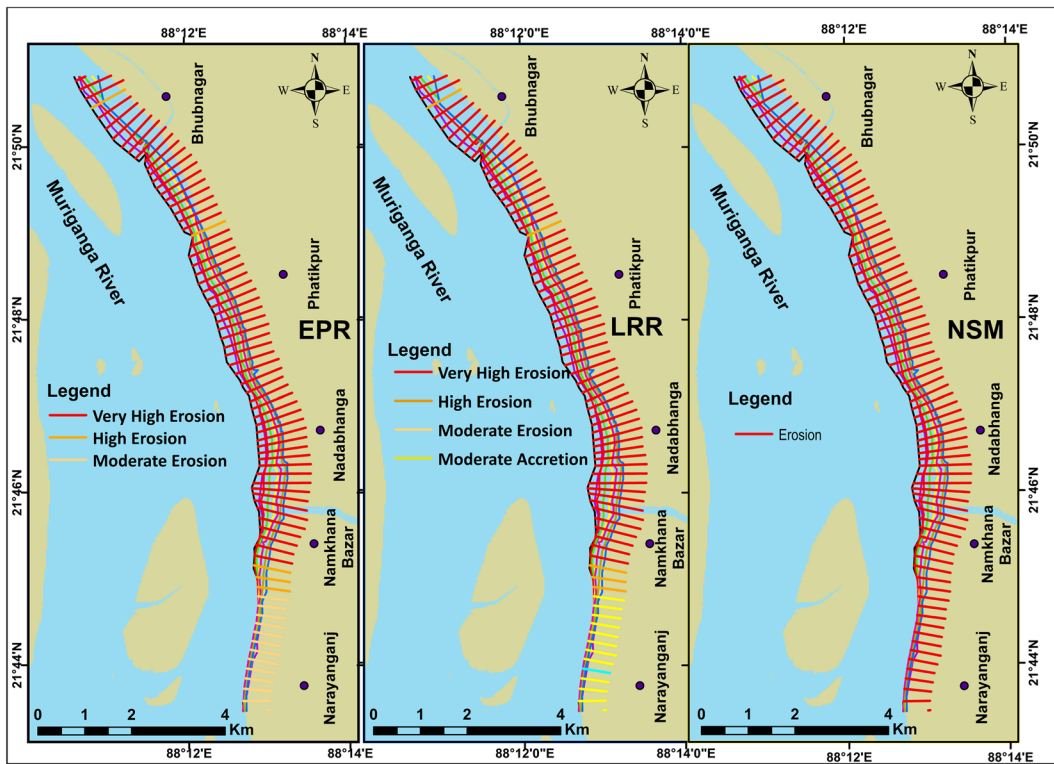
Fig. 19 Assessments of different degrees of erosion–accretion in the Namkhana sector during the time period of 1972 to 2021 from EPR, LRR and NSM

3–8 mm/year (Raha et al., 2014). Apart from the sea-level rise, there is a continuous increase in wave height and wave form velocity (Paul, 2002; Purkait, 2009). These factors are mainly responsible for the coastal erosion of Sagar island. The southeastern, southwestern and the northeastern sides of the Sagar island are subjected to severe erosion (Fig 4). Moreover, the popular navigational active channels like Rangafalla, Jhelingham, Eden and Auckland are located on the western side of Sagar island. These channels are dredged occasionally to maintain the navigability. As a result, there may be a chance that the western side of the Sagar island gets eroded. Previous studies by Gopinath and Seralathan (2005) and Jayappa et al. (2006) also found that the above said region of Sagar island is subjected to enormous erosion.

Though the higher sand content is found in the western side, on the eastern side, the sediments are predominately silt (Gopinath & Seralathan, 2005). They found that the erosion for the last 32 years, starting from 1967 to 1999, was 16.9 km^2 (1690 ha). Similarly, this study found that the erosion for 32 years starting from 1972 to 2004 is 1670.63 ha (Table 3). From the comparison, it can be said that the results are comparable. This island shows more accretion during 1996–2004 and 2004–2011 time periods in short-term analysis (Fig. 4b), and the maximum erosion is found during the period of 2017–2021. This is probably due to the super cyclone Amphan (2020) causes landfall near Sagar island (Bhattacharjee & Dhara, 2021).

The Ghoramara island has lost almost 50% of its area within last five decades. This island is shrinking continuously without changing its shape. Higher erosion has taken place in the northwest (NW) side, whereas the lower rate of erosion is found in the southeast side. One of the possible reasons for higher erosion in the NW side is that it gets the direct hit of the tidal flow during the ebb tide of the Hooghly river with full energy (Ghosh et al., 2003; Adarsa et al., 2012). Another factor may be the sea-level rise
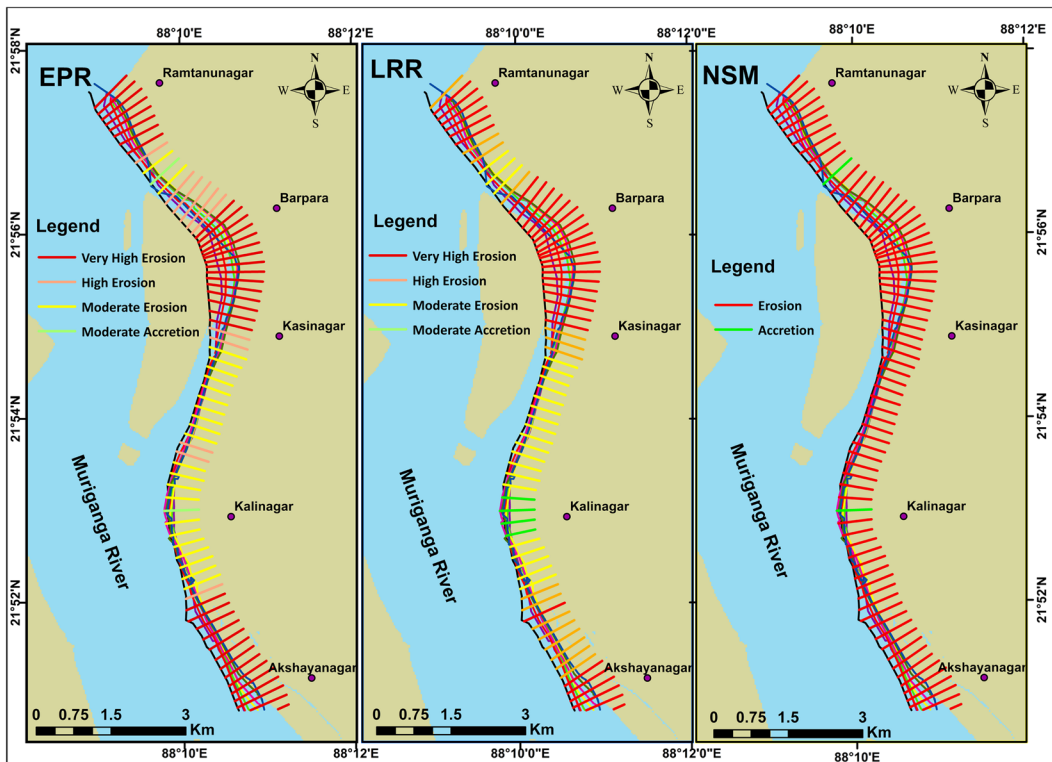
Fig. 20 Assessments of different degrees of erosion–accretion in the Kakdwip sector during the time period of 1972 to 2021 from EPR, LRR and NSM
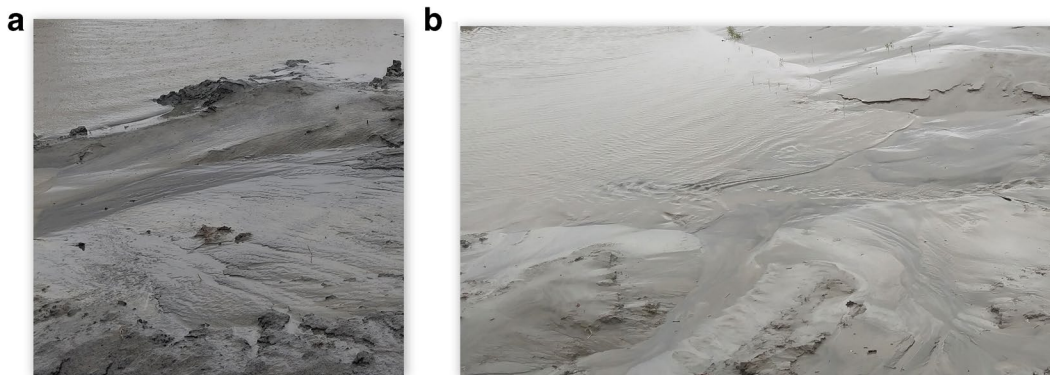

Fig. 21 Tidal flats on the left bank of the Muriganga River at the Kakdwip sector near Akshyanagar (a) and Kalinagar (b)

as it may accelerate the erosion at the northwestern part of the island, while it acts as a retarding factor to the accretion at the southeastern part (Ghosh et al., 2003). The tidal force does hardly hits this island as it lies near the shadow zone of Sagar island. Erosion on the NW side and accretion on the southern side are observed during 1972–1980 (Fig. 5). Adarsa et al. (2012) observed that the net erosion during 1972–2010 was 428.6 ha. This study also found that the net erosion during the period of 1972–2011 is

Fig. 22 Erosion at the Kakdwip sector near Kalinagar

430.42 ha. The maximum erosion rates of 17.74 ha/year and 16.54 ha/year have been observed during the period of 1972–1980 and 1980–1988, respectively.

The northern region of the river experiences strong micro-tidal currents due to active river flow, whereas the southern region is experiencing strong tidal wave (Ghosh & Mukhopadhyay, 2016). This could be

Fig. 23 Mud decoupling at the toe on the left bank near Akshyanagar

Fig. 24 Wooden embankment and brick kiln at the Kakdwip sector

the reason that the islands which are located in the upstream reach, such as Basit and Niogi islands, are getting accreted. The Mousuni and Pushpa islands, located downstream of the reach, are continuously losing their area. The Half-fish island is the most dynamic island in the Muriganga River, which is also continuously shrinking till 2004, but in 2011, it again accumulated a significant area. Cyclones can bring extremely high wind, heavy rainfall and high tidal surge, which can erode the shoreline within a shorter period of time. Major cyclones like Aila (2009), Fani (2019), Bulbul (2019) and Amphan (2020) have been found in this coastal region. Islands like Sagar, Ghoramara, Mousuni and Pushpa are getting eroded continuously.

Conclusion

With the help of remote sensing and geospatial techniques along with DSAS 5.0, the morphological changes in Sagar island, Ghoramara island and Muriganga River as well as in its islands are analysed using the 8 cloud-free Landsat images starting from 1972 to 2021. The water body and land were differentiated with the help of NDWI. The area of each islands were computed from each Landsat image. The LRR, EPR and NSM were found with the help of DSAS 5.0. As stated earlier, mainly, the islands in the upper region are subjected to accretion, whereas those in the lower region are subjected to erosion. This is possibly due to the effect of tidal force which is generally more impactful in the lower region of the estuary. Similarly, the upper region may be accreted due to the accumulation of the sediments carried from the upstream of the Hooghly river and eroded materials of the river banks and Ghoramara islands.

From the analysis, it is found that both the banks of the Muriganga River are eroding at an average rate of about 5 m/year (left bank) and 3 m/year (right bank). The higher erosion is found in the left bank possibly, due to the convexity of the bank line. Moreover, the analysis indicates that the Sagar, Ghoramara, Pushpa and Mousuni islands are continuously eroding. The remaining islands such as Basit, Niogi and Half-fish are expanding their area.

Shoreline erosion is one of the vital threats to the people living near the bank. The properties,

buildings and agriculture land can be lost due to erosion. The habitats loss can affect the wildlife, birds, plants and animals also. The eroded materials which are carried out by the river can disrupt the aquatic environment. Moreover, the damaged caused by erosion can lead to very high expenses. Rebuilding and repairing of infrastructures and roads, compensating with property owners etc., are quite expensive. This study found that some places on both the left and right banks are vulnerable due to erosion. All sides of Ghoramara island, the western and southern sides of Sagar island, the western side of Mousuni island and the left bank of the Muriganga River are of great concern. Particularly Dhablat, Khasmahal, between Chemaguri and Benuban, Bankimnagar, Mrityunjoynagar, Bamankhai, Bakultala, Kastala, Fraserganj, Patibunia, between Janamore and Debnagar, Namkhana Bazar, Nadabhanga, Phatikpur, Bhubnagar, Akshaynagar, Barpara and Ramtanunagar are the erodible areas where more attention is needed.

Effective coastal management techniques are crucial for lowering the dangers caused by either natural or human-made activities. If the precautions are not taken, the people living on the edges may face many difficulties. As mentioned earlier, it is found that in the area where local authorities have taken some measures (Fig. 24), the erosion due to fluvial and other natural activities has reduced substantially. This study will be helpful in implementing the coastal management technique to prevent bank erosion in the area where the current erosion rate is high, as identified by this study and written in the previous paragraph.

From the study, it is clear that the Pushpa island is diminishing day by day. Along with that, the Ghoramara island has lost almost half of its area with last five decades. Similarly, popular islands like Sagar and Mousuni have also lost an adequate amount of their area. Again, the evolution of a new island (i.e. Niogi) within the river body would disrupt the aquatic life. In addition, the hydrodynamic and sediment transport modelling can be performed to study how the hydrodynamic forces such as tides, wind and wave can influence the shoreline shifting. The sediment model can help in finding the erosion–deposition process by proving the location where the erosion and deposition have taken place.

with the Landsat images. We acknowledge with gratitude the facilities and infrastructure provided by the Civil Engineering Department, Indian Institute of Engineering Science and Technology (IIEST), Shibpur.

References

Adarsa, J., Shamina, S., & Arkoprovo, B. (2012). Morphological change study of Ghoramara Island, Eastern India using multi temporal satellite data. *Research Journal of Recent Sciences Res.J.Recent Science, 1*(10), 72–81.

Aladwani, N. S. (2022). Shoreline change rate dynamics analysis and prediction of future positions using satellite imagery for the southern coast of Kuwait: A case study. *Oceanologia.* https://doi.org/10.1016/j.oceano.2022.02.002

Amin, S. M. N., & Davidson-Arnott, R. G. D. (1997). A statistical analysis of the controls on shoreline erosion rates, Lake Ontario. *Journal of Coastal Research, 13*(4), 1093–1101.

Bagli, S., & Soille, P. (2003). Morphological automatic extraction of Pan-European coastline from Landsat ETM+ images. In *International Symposium on GIS and Computer Cartography for Coastal Zone Management.*

Bakshi, S., & Bhar, K. K. (2020). Simulation of tidal morphodynamics in the Hooghly Estuary using CMS flow and artificial neural network models. *Procedia Computer Science, 167*(2019), 459–467. https://doi.org/10.1016/j.procs.2020.03.255

Bandyopadhyay, S., Mukherjee, D., & Bag, S. (2004). 20th century evolution of banks and islands of the Hugli Estuary, West Bengal, India: Evidence from maps. *Images and GPS Survey.* https://doi.org/10.5281/zenodo.7264822

Bera, A., Meraj, G., Kanga, S., Farooq, M., Singh, S. K., Sahu, N., & Kumar, P. (2022). Vulnerability and risk assessment to climate change in Sagar Island, India. *Water (Switzerland), 14*(5). https://doi.org/10.3390/w14050823

Bhattacharjee, A., & Dhara, S. (2021). Natural hazards and disasters: Management at Sagar island of South 24 Parganas District, *9*(1), 4571–4578.

Broers, H. P., Peters, S. W. M., & Biesheuvel, A. (1990). Design of a groundwater quality monitoring network with GIS and remote sensing. *Proceedings of the first European conference on geographic information systems, EGIS, 90,* 95–106.

Chakraborty, S. (2013). Delineation of morpho-structural changes of some selected islands in the Ganga delta region, West Bengal, India – A spatio-temporal change detection analysis using GIS and remote sensing, *4*(3), 499–507. https://doi.org/10.13140/RG.2.1.2865.8161

Chrisben Sam, S., & Gurugnanam, B. (2022). Coastal transgression and regression from 1980 to 2020 and shoreline forecasting for 2030 and 2040, using DSAS along the southern coastal tip of Peninsular India. *Geodesy and Geodynamics.* https://doi.org/10.1016/j.geog.2022.04.004

Crowell, M., Douglas, B. C., & Leatherman, S. P. (1997). On forecasting future U.S. shoreline positions: A test of algorithms. *Journal of Coastal Research, 13*(4), 1245–1255.

Dépret, T., Gautier, E., Hooke, J., Grancher, D., Virmoux, C., & Brunstein, D. (2017). Causes of planform stability of a low-energy meandering gravel-bed river (Cher River, France). *Geomorphology, 285,* 58–81. https://doi.org/10.1016/j.geomorph.2017.01.035

Demir, H., Otay, E. N., Work, P. A., & Börekçi, O. S. (2004). Impacts of dredging on shoreline change. J. *Waterw. Port, Coast. Ocean Engineering, 130*(4), 170–178. https://doi.org/10.1061/(ASCE)0733-950X(2004)130:4(170)

Dilara, C., & Tarik, T. (2019). Automatic detection of shoreline change by geographical information system (GIS) and remote sensing in the Göksu Delta, Turkey. *Journal of the Indian Society of Remote Sensing, 47*(2), 233–243. https://doi.org/10.1007/s12524-019-00947-1

Ding, Y., & Wang, S. S. Y. (2008). Development and application of a coastal and estuarine morphological process modeling system. *Journal of Coastal Research, 10052*(10052), 127–140. https://doi.org/10.2112/1551-5036-52.sp1.127

Dixon, S. J., Smith, G. H. S., Best, J. L., Nicholas, A. P., Bull, J. M., Vardy, M. E., Sarker, M. H., & Goodbred, S. (2018). The planform mobility of river channel confluences: *Insights from analysis of remotely sensed imagery. Earth-Science Reviews, 176,* 1–18. https://doi.org/10.1016/j.earscirev.2017.09.009

Dolan, R., Fenster, M. S., & Holme, S. J. (1991). Florida accretion. *Journal of Coastal Research, 7*(3), 723–744.

Dubey, R. P., Samarawickrama, S., Gunaratna, P. P., Halgahawatta, L., Pathirana, K. P. P., Raveenthiran, K., et al. (2014). Mathematical model studies for river regulatory measures for the improvement of draft in Hoogly Estuary, India. *International Journal of Engineering and Technologies, 2,* 1–12. https://doi.org/10.56431/p-740099

Dutta, D., Kumar, T., Jayaram, C., & Akram, W. (2022). Shoreline change analysis of Hooghly Estuary using multi-temporal Landsat data and digital shoreline analysis system. *Geographic Information Systems and Applications in Coastal Studies, 1–37.* https://doi.org/10.5772/intechopen.103030

Ghosh, A., & Mukhopadhyay, S. (2016). Quantitative study on shoreline changes and erosion hazard assessment: Case study in Muriganga–Saptamukhi interfluve, Sundarban,

India. *Modeling Earth Systems and Environment, 2*(2), 1–14. https://doi.org/10.1007/s40808-016-0130-x

Ghosh, T., Bhandari, G., & Hazra, S. (2003). Application of a "bio-engineering" technique to protect Ghoramara Island (Bay of Bengal) from severe erosion. *Journal of Coastal Conservation, 9*(2), 171–178. https://doi.org/10.1652/1400-0350(2003)009[0171:AOABTT]2.0.CO;2

Gopinath, G., & Seralathan, P. (2005). Rapid erosion of the coast of Sagar island, West Bengal - India. *Environmental Geology, 48*(8), 1058–1067. https://doi.org/10.1007/s00254-005-0044-9

Gratiot, N., Anthony, E. J., Gardel, A., Gaucherel, C., Proisy, C., & Wells, J. T. (2008). Significant contribution of the 18.6 year tidal cycle to regional coastal changes. *Nature Geoscience, 1*(3), 169–172. https://doi.org/10.1038/ngeo127

Hakkou, M., Maanan, M., Belrhaba, T., El Khalidi, K., El Ouai, D., & Benmohammadi, A. (2018). Multi-decadal assessment of shoreline changes using geospatial tools and automatic computation in Kenitra coast, Morocco. *Ocean and Coastal Management, 163*, 232–239. https://doi.org/10.1016/j.ocecoaman.2018.07.003

Hassan, A., Martin, T. C., & Mosselman, E. (1999). Island topography mapping for the Brahmaputra-Jamuna River using remote sensing and GIS. *Geological Society Special Publication, 163*, 153–161. https://doi.org/10.1144/GSL.SP.1999.163.01.13

Hazra, S., Ghosh, T., Dasggupta, R., & Sen, G. (2002). Sea level and associated changes in sundarban. *Science and Culture, 68*(9), 309–321.

Himmelstoss, E. A., Henderson, R. E., Kratzmann, M. G., & Farris, A. S. (2018). Digital Shoreline Analysis System (DSAS) Version 5.0 User Guide. *U.S. Geological Survey Open-File Report 2018–1179*, 1–104.

Islam, M. N. (2000). *Braiding and channel morphodynamics: The Brahmaputra-Jamuna river, Bangladesh.* Doctoral dissertation, University of Hull.

Jayakumar, K., & Malarvannan, S. (2016). Assessment of shoreline changes over the Northern Tamil Nadu Coast, South India using WebGIS techniques. *Journal of Coastal Conservation, 20*(6), 477–487. https://doi.org/10.1007/s11852-016-0461-9

Jayappa, K. S., Mitra, D., & Mishra, A. K. (2006). Coastal geomorphological and land-use and land-cover study of Sagar Island, Bay of Bengal (India) using remotely sensed data. *International Journal of Remote Sensing, 27*(17), 3671–3682. https://doi.org/10.1080/01431160500500375

Jones, R., Bessell-Browne, P., Fisher, R., Klonowski, W., & Slivkoff, M. (2016). Assessing the impacts of sediments from dredging on corals. *Marine Pollution Bulletin, 102*(1), 9–29. https://doi.org/10.1016/j.marpolbul.2015.10.049

Kumar, A., & Jayappa, K. S. (2009). Long and short-term shoreline changes along Mangalore coast, India. *International Journal of Environmental Research, 3*(2), 177–188.

Knighton, D. (1984). *Fluvial forms and processes* (p. 218). Edward Arnold.

Laha, C., & Bandyapadhyay, S. (2013). Analysis of the changing morphometry of River Ganga, shift monitoring and vulnerability analysis using space-borne techniques: A

statistical approach. *International Journal of Scientific and Research Publications, 3*(7), 1–10.

Maheshvaran, V., Murali, K., Sundar, V., & Chitra, K. (2019). Study on maintenance dredging for navigable depth assurance in the macro-tidal hooghly estuary. *Lecture Notes in Civil Engineering, 23*, 353–367. https://doi.org/10.1007/978-981-13-3134-3_27

Maiti, S., & Bhattacharya, A. K. (2009). Shoreline change analysis and its application to prediction: A remote sensing and statistics based approach. *Marine Geology, 257*(1–4), 11–23. https://doi.org/10.1016/j.margeo.2008.10.006

Marcus, W. A., & Fonstad, M. A. (2010). Remote sensing of rivers: The emergence of a subdiscipline in the river sciences. *Earth Surface Processes and Landforms, 35*(15), 1867–1872. https://doi.org/10.1002/esp.2094

Marfai, M. A., & Almohammad, H. (2008). *Coastal dynamic and shoreline mapping: Multi-sources spatial data analysis in Semarang Indonesia* (pp. 297–308). https://doi.org/10.1007/s10661-007-9929-2

Mcbride, R. A., Byrnes, M. R., & Hiland, M. W. (1995). Geomorphic response-type model for barrier coastlines: A regional perspective. *Marine Geology, 126*(1-4), 143–159.

McFeeters, S. K. (1996). The use of the normalized difference water index (NDWI) in the delineation of open water features. *International Journal of Remote Sensing, 17*(7), 1425–1432. https://doi.org/10.1080/01431169608948714

Mills, J. P., Buckley, S. J., Mitchell, H. L., Clarke, P. J., & Edwards, S. J. (2005). A geomatics data integration technique for coastal change monitoring, *664*, 651–664. https://doi.org/10.1002/esp.1165

Monge-Ganuzas, M., Cearreta, A., & Evans, G. (2013). Morphodynamic consequences of dredging and dumping activities along the lower Oka estuary (Urdaibai Biosphere Reserve, southeastern Bay of Biscay, Spain). *Ocean and Coastal Management, 77*, 40–49. https://doi.org/10.1016/j.ocecoaman.2012.02.006

Morisawa, M., & Hack, J. T. (1985). Tectonic geomorphology. In *Proceedings of the 15th Annual Binghamton Geomorphology Symposium. September 1984*. Allen and Unwin xiv + 390.

Morris, R. (2007). A nature conservation perspective of port-related dredging. Proceedings of the Institution of Civil Engineers. *Maritime Engineering, 160*(1), 19–23. https://doi.org/10.1680/maen.2007.160.1.19

Mount, N. J., Tate, N. J., Sarker, M. H., & Thorne, C. R. (2013). Evolutionary, multi-scale analysis of river bank line retreat using continuous wavelet transforms: Jamuna River, Bangladesh. *Geomorphology, 183*, 82–95. https://doi.org/10.1016/j.geomorph.2012.07.017

Mujabar, P. S., & Chandrasekar, N. (2011). Shoreline change analysis along the coast between Kanyakumari and Tuticorin of India using remote sensing and GIS. *Arabian Journal of Geosciences, 6*(3), 647–664. https://doi.org/10.1007/s12517-011-0394-4

Mukherjee, K. N. (1983). History of settlement in the Sundarbans. *Indian Journal of Landscape Systems and Ecological Studies, 6*, 1–19.

Mukhopadhyay, A., Mukherjee, S., Hazra, S., & Mitra, D. (2011). Sea level rise and shoreline changes: A geoinformatic appraisal of Chandipur Coast, Orissa. *International*

Journal of Geology, Earth and Environmental Sciences, 1(1), 9–17.

Muthusankar, G. (2011). *Multi hazard risk assessment and management strategies for Nagapattinam Coastal Zone, Tamil Nadu* (p. 147). Bharathidasan University. Ph.D thesis http://14.139.186.108/jspui/bitstream/123456789/31181/1/Muthusankar_Ph.D.thesis.pdf.

Nandi, S., Ghosh, M., Kundu, A., Dutta, D., & Baksi, M. (2016). Shoreline shifting and its prediction using remote sensing and GIS techniques: A case study of Sagar Island, West Bengal (India). *Journal of Coastal Conservation, 20*(1), 61–80. https://doi.org/10.1007/s11852-015-0418-4

Nassar, K., Mahmod, W. E., Fath, H., Masria, A., Nadaoka, K., & Negm, A. (2018). Shoreline change detection using DSAS technique: Case of North Sinai coast, Egypt. *Marine Georesources and Geotechnology, 37*(1), 81–95. https://doi.org/10.1080/1064119X.2018.1448912

Natarajan, L., Sivagnanam, N., Usha, T., Chokkalingam, L., Sundar, S., Gowrappan, M., & Roy, P. D. (2021). Shoreline changes over last five decades and predictions for 2030 and 2040: A case study from Cuddalore, southeast coast of India. *Earth Science Informatics, 14*(3), 1315–1325. https://doi.org/10.1007/s12145-021-00668-5

Nithu, R. R., Rejin Nishkalank, A., & Chrisben Sam, S. (2020). Coastal shoreline changes in Chennai: Environment impacts and control strategies of southeast coast Tamil Nadu. *Handbook Environ Mater Manag.* https://doi.org/10.1007/978-3-319-58538-3_223-1

Purkait, B. (2009). Coastal erosion in response to wave dynamics operative in Sagar Island, Sundarban delta, India. *Frontiers of Earth Science in China, 3*(1), 21–33. https://doi.org/10.1007/s11707-009-0001-0

Raha, A. K., Mishra, A., Bhattacharya, S., Ghatak, S., Pramanick, P., Dey, S., Sarkar, I., & Jha, C. (2014). Sea level rise and submergence of Sundarban islands: a time series study of estuarine dynamics. *Journal of Ecology and Environmental Sciences, 5*(1), 114–123. http://www.bioinfopublication.org/jouarchive.php?opt=&jouid=BPJ0000261

Roberts, G., France, M., Johnson, R. C., & Law, J. T. (1993). The analysis of remotely sensed images of the Balquhidder catchments for estimation of percentages of land cover types. *Journal of Hydrology, 145*(3–4), 259–265. https://doi.org/10.1016/0022-1694(93)90058-H

Saichenthur, N., Murali, K., & Sundar, V. (2021). Studies on locating sediment trap for reducing dredging in Jellingham Navigational Fairway, Kolkata. In *Lecture Notes in Civil Engineering* (Vol. *106*, pp. 185–199). https://doi.org/10.1007/978-981-15-8506-7_15

Salghuna, N. N., & Bharathvaj, S. A. (2015). Shoreline change analysis for northern part of the Coromandel Coast.

Aquatic Procedia, 4, 317–324. https://doi.org/10.1016/j.aqpro.2015.02.043

Saranathan, E., Chandrasekaran, R., Manickaraj, D. S., & Kannan, M. (2011). Shoreline changes in Tharangampadi Village, Nagapattinam District, Tamil Nadu, India- A case study. *Journal of the Indian Society of Remote Sensing, 39*(1), 107–115. https://doi.org/10.1007/s12524-010-0052-4

Sarker, M. H., & Thorne, C. R. (2009). Morphological response of the Brahmaputra–Padma–Lower Meghna river system to the Assam Earthquake of 1950. *Braided Rivers*, 289–310. https://doi.org/10.1002/9781444304374.ch14

Scott, D. B. (2005). Coastal changes, rapid. In M. L. Schwartz (Ed.), *Encyclopedia of coastal sciences* (pp. 253–255). Springer.

Sunarto, S. (2004). *Geomorphic changes in coastal area surround Muria Volcano.* Gadjah Mada University Yogyakarta.

Thieler, E. R., Himmelstoss, E. A., Zichichi, J. L., & Ergul, A. (2009). The digital shoreline analysis system (DSAS) version 4.0—An ArcGIS extension for calculating shoreline change. In *Open-File Report, US Geological Survey Report No. 2008-1278*.

Thom, B. G., & Cowell, P. J. (2005). Coastal changes, gradual. In M. L. Schwartz (Ed.), *Encyclopedia of coastal sciences* (pp. 251–253). Springer.

Wiel, M. J. Van De. (2003). University of Southampton numerical modelling of channel adjustment in alluvial meandering rivers with riparian vegetation. A thesis submitted for the degree of Doctor of Philosophy Faculty of Science Department of Geography July 20, 4(July)

Wright, L. D., & Coleman, J. M. (1973). Variations in morphology of major river deltas as functions of ocean wave and river discharge regimes. *American Association of Petroleum Geologists Bulletin, 57*(2), 370–398. https://doi.org/10.1306/819a4274-16c5-11d7-8645000102c1865d

Zhang, K., Douglas, B. C., & Leatherman, S. P. (2004). Global warming and coastal erosion. *Climatic change, 64*, 41–58.